Recent measurement and experimental prospects of the Muon *g-2* experiment at Fermilab

E. Bottalico

EINN 2023

31 October 2023

The history of Muon g-2

The history of the Muon g-2 experiments finds its roots in the series of experiment at CERN

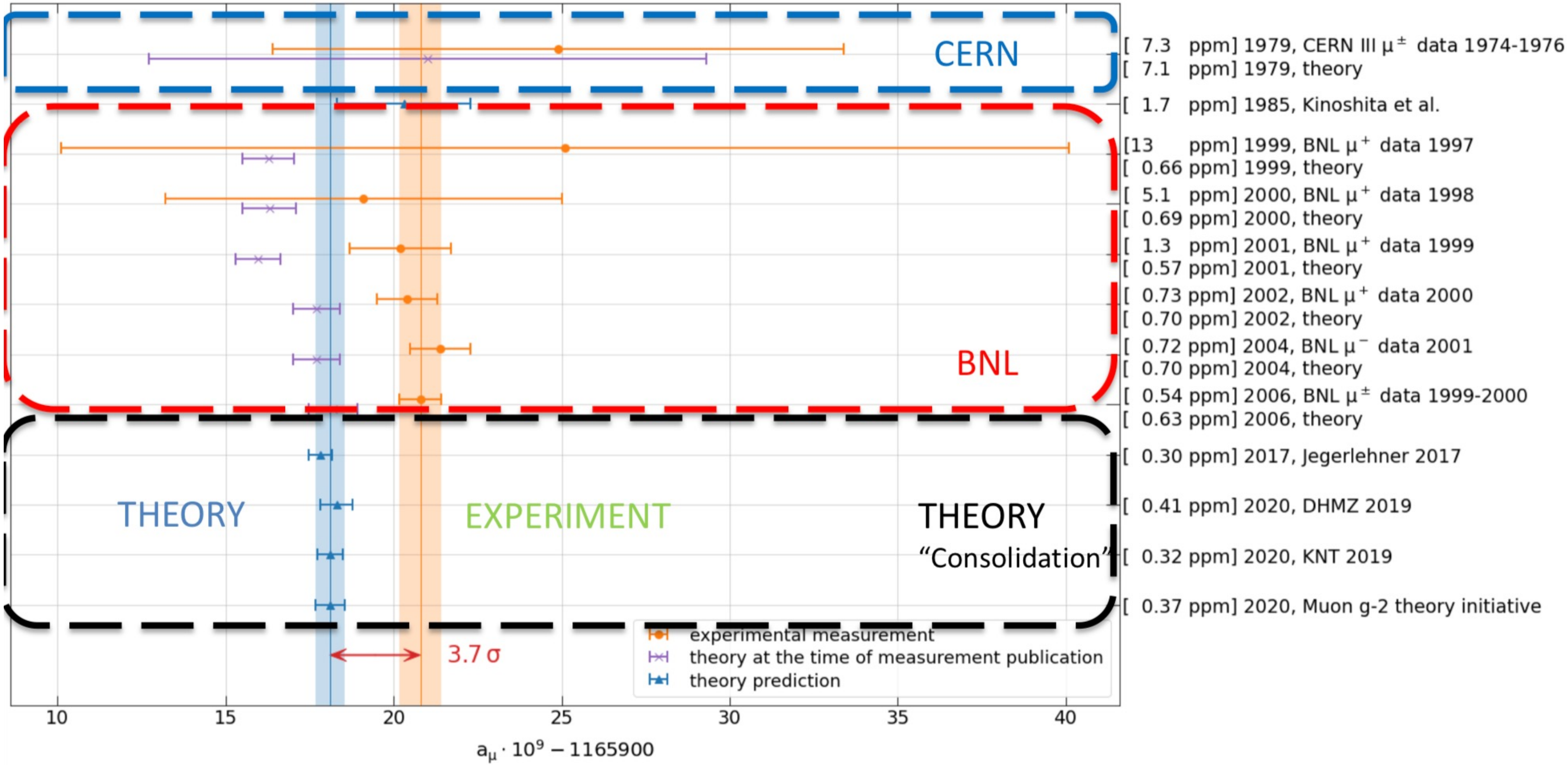

Muon g-2 today: Data collection

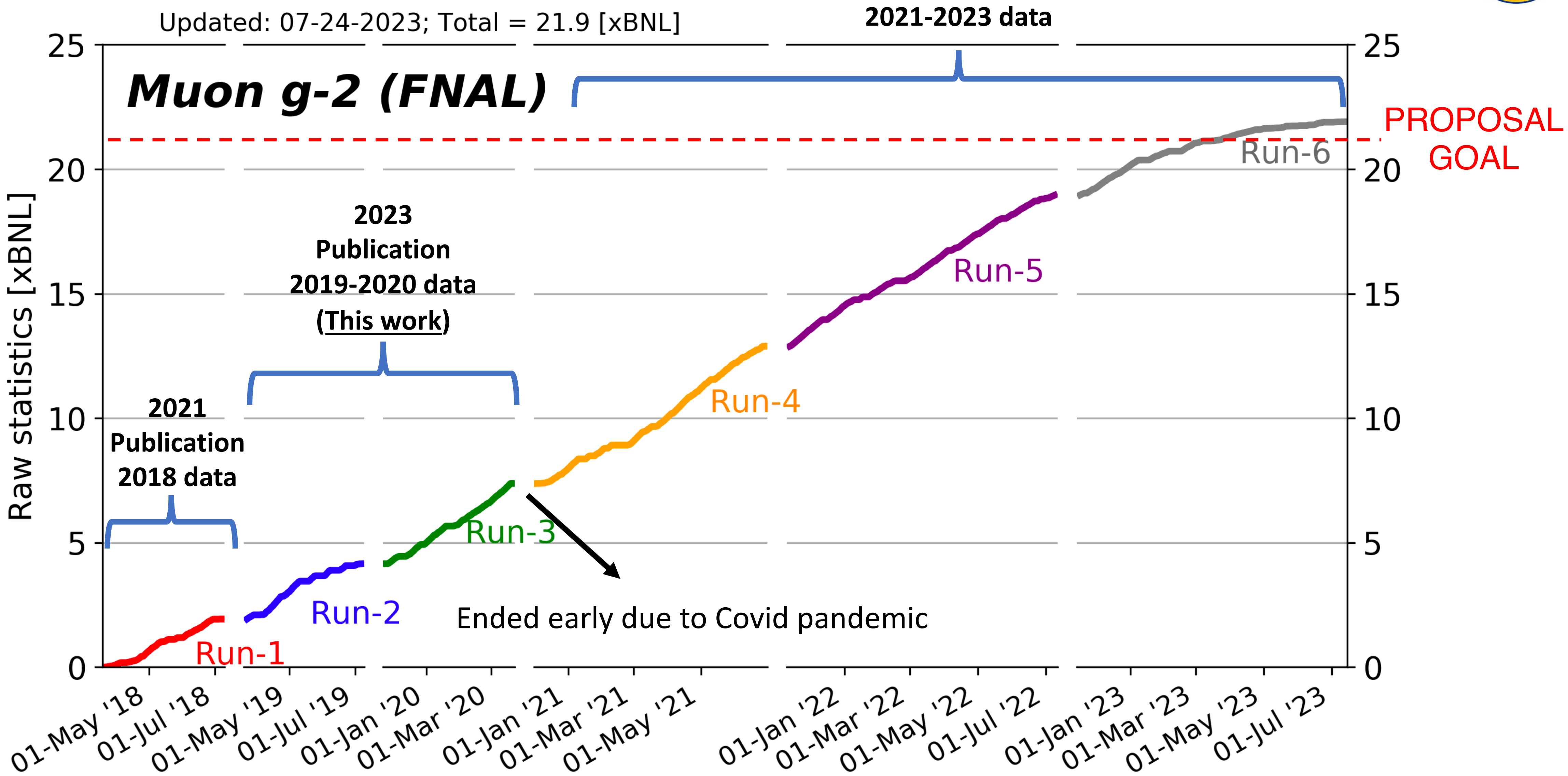

Run-1 Publication

Published on PRL – 7th April 2021

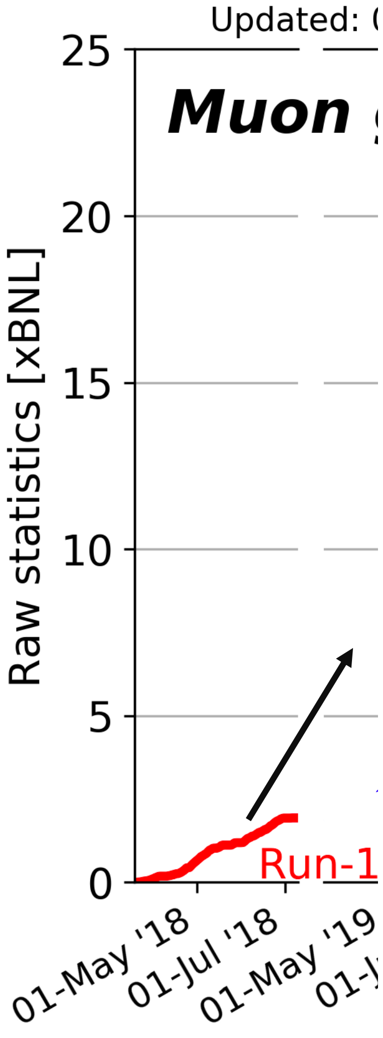

31/10/23

Measurement of the Positive Muon Anomalous Magnetic Moment to 0.46 ppm

B. Abi,[44] T. Albahri,[39] S. Al-Kilani,[36] D. Allspach,[7] L. P. Alonzi,[48] A. Anastasi,[11,a] A. Anisenkov,[4,b] F. Azfar,[44] K. Badgley,[7] S. Baeßler,[47,c] I. Bailey,[19,d] V. A. Baranov,[17] E. Barlas-Yucel,[37] T. Barrett,[6] E. Barzi,[7] A. Basti,[11,32] F. Bedeschi,[11] A. Behnke,[22] M. Berz,[20] M. Bhattacharya,[43] H. P. Binney,[48] R. Bjorkquist,[6] P. Bloom,[21] J. Bono,[7] E. Bottalico,[11,32] T. Bowcock,[39] D. Boyden,[22] G. Cantatore,[13,34] R. M. Carey,[2] J. Carroll,[39] B. C. K. Casey,[7] D. Cauz,[35,8] S. Ceravolo,[9] R. Chakraborty,[38] S. P. Chang,[18,5] A. Chapelain,[6] S. Chappa,[7] S. Charity,[7] R. Chislett,[36] J. Choi,[5] Z. Chu,[26,e] T. E. Chupp,[42] M. E. Convery,[7] A. Conway,[41] G. Corradi,[9] S. Corrodi,[1] L. Cotrozzi,[11,32] J. D. Crnkovic,[3,37,43] S. Dabagov,[9,f] P. M. De Lurgio,[1] P. T. Debevec,[37] S. Di Falco,[11] P. Di Meo,[10] G. Di Sciascio,[12] R. Di Stefano,[10,30] B. Drendel,[7] A. Driutti,[35,13,38] V. N. Duginov,[17] M. Eads,[22] N. Eggert,[6] A. Epps,[22] J. Esquivel,[7] M. Farooq,[42] R. Fatemi,[38] C. Ferrari,[11,14] M. Fertl,[48,16] A. Fiedler,[22] A. T. Fienberg,[48] A. Fioretti,[11,14] D. Flay,[41] S. B. Foster,[2] H. Friedsam,[7] E. Frlež,[47] N. S. Froemming,[48,22] J. Fry,[47] C. Fu,[26,e] C. Gabbanini,[11,14] M. D. Galati,[11,32] S. Ganguly,[37,7] A. Garcia,[48] D. E. Gastler,[2] J. George,[41] L. K. Gibbons,[6] A. Gioiosa,[29,11] K. L. Giovanetti,[15] P. Girotti,[11,32] W. Gohn,[38] T. Gorringe,[38] J. Grange,[1,42] S. Grant,[36] F. Gray,[24] S. Haciomeroglu,[5] D. Hahn,[7] T. Halewood-Leagas,[39] D. Hampai,[9] F. Han,[38] E. Hazen,[2] J. Hempstead,[48] S. Henry,[44] A. T. Herrod,[39,d] D. W. Hertzog,[48] G. Hesketh,[36] A. Hibbert,[39] Z. Hodge,[48] J. L. Holzbauer,[43] K. W. Hong,[47] R. Hong,[1,38] M. Iacovacci,[10,31] M. Incagli,[11] C. Johnstone,[7] J. A. Johnstone,[7] P. Kammel,[48] M. Kargiantoulakis,[7] M. Karuza,[13,45] J. Kaspar,[48] D. Kawall,[41] L. Kelton,[38] A. Keshavarzi,[40] D. Kessler,[41] K. S. Khaw,[27,26,48,e] Z. Khechadoorian,[6] N. V. Khomutov,[17] B. Kiburg,[7] M. Kiburg,[7,21] O. Kim,[18,5] S. C. Kim,[6] Y. I. Kim,[5] B. King,[39,a] N. Kinnaird,[2] M. Korostelev,[19,d] I. Kourbanis,[7] E. Kraegeloh,[42] V. A. Krylov,[17] A. Kuchibhotla,[37] N. A. Kuchinskiy,[17] K. R. Labe,[6] J. LaBounty,[48] M. Lancaster,[40] M. J. Lee,[5] S. Lee,[5] S. Leo,[37] B. Li,[26,1,e] D. Li,[26,g] L. Li,[26,e] I. Logashenko,[4,b] A. Lorente Campos,[38] A. Lucà,[7] G. Lukicov,[36] G. Luo,[22] A. Lusiani,[11,25] A. L. Lyon,[7] B. MacCoy,[48] R. Madrak,[7] K. Makino,[20] F. Marignetti,[10,30] S. Mastroianni,[10] S. Maxfield,[39] M. McEvoy,[22] W. Merritt,[7] A. A. Mikhailichenko,[6,a] J. P. Miller,[2] S. Miozzi,[12] J. P. Morgan,[7] W. M. Morse,[3] J. Mott,[2,7] E. Motuk,[36] A. Nath,[10,31] D. Newton,[39,a,d] H. Nguyen,[7] M. Oberling,[1] R. Osofsky,[48] J.-F. Ostiguy,[7] S. Park,[5] G. Pauletta,[35,8] G. M. Piacentino,[29,12] R. N. Pilato,[11,32] K. T. Pitts,[37] B. Plaster,[38] D. Počanić,[47] N. Pohlman,[22] C. C. Polly,[7] M. Popovic,[7] J. Price,[39] B. Quinn,[43] N. Raha,[11] S. Ramachandran,[1] E. Ramberg,[7] N. T. Rider,[6] J. L. Ritchie,[46] B. L. Roberts,[2] D. L. Rubin,[6] L. Santi,[35,8] D. Sathyan,[2] H. Schellman,[23,h] C. Schlesier,[37] A. Schreckenberger,[46,2,37] Y. K. Semertzidis,[5,18] Y. M. Shatunov,[4] D. Shemyakin,[4,b] M. Shenk,[22] D. Sim,[39] M. W. Smith,[48,11] A. Smith,[39] A. K. Soha,[7] M. Sorbara,[12,33] D. Stöckinger,[28] J. Stapleton,[7] D. Still,[7] C. Stoughton,[7] D. Stratakis,[7] C. Strohman,[6] T. Stuttard,[36] H. E. Swanson,[48] G. Sweetmore,[40] D. A. Sweigart,[6] M. J. Syphers,[22,7] D. A. Tarazona,[20] T. Teubner,[39] A. E. Tewsley-Booth,[42] K. Thomson,[39] V. Tishchenko,[3] N. H. Tran,[2] W. Turner,[39] E. Valetov,[20,19,27,d] D. Vasilkova,[36] G. Venanzoni,[11] V. P. Volnykh,[17] T. Walton,[7] M. Warren,[36] A. Weisskopf,[20] L. Welty-Rieger,[7] M. Whitley,[39] P. Winter,[1] A. Wolski,[39,d] M. Wormald,[39] W. Wu,[43] and C. Yoshikawa[7]

(Muon $g-2$ Collaboration)

Quantity	Correction terms (ppb)	Uncertainty (ppb)
ω_a^m (statistical)	⋯	434
ω_a^m (systematic)	⋯	56
C_e	489	53
C_p	180	13
C_{ml}	−11	5
C_{pa}	−158	75
$f_{\text{calib}}\langle\omega_p(x,y,\phi)\times M(x,y,\phi)\rangle$	⋯	56
B_k	−27	37
B_q	−17	92
$\mu_p'(34.7°)/\mu_e$	⋯	10
m_μ/m_e	⋯	22
$g_e/2$	⋯	0
Total systematic	⋯	157
Total fundamental factors	⋯	25
Totals	544	462

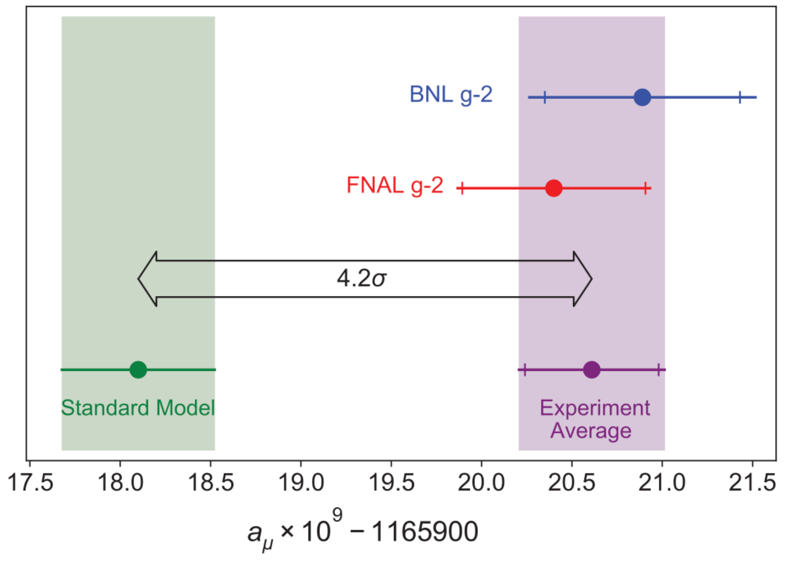

What is the Muon g-2?

The intrinsic magnetic moment of a particle with spin is:

$$\vec{\mu} = g\frac{q}{2m}\vec{S}$$

The g-factor (gyromagnetic) defines the coupling between the spin and the magnetic field:

- g = 1 classic theory;
- g = 2 Dirac quantum theory;
- g = 2.00233… quantum field theory.

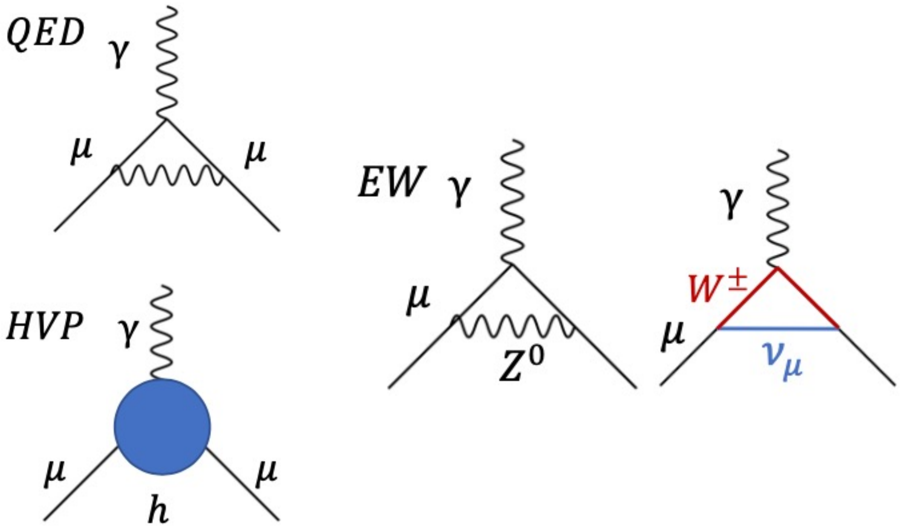

How do we measure a_μ?

- Muons are injected in a magnetic field of **1.45 T**
- When a muon moves in a uniform magnetic field its spin rotates faster than its momentum (if **g>2**) and the difference between the spin and momentum angular velocity is the anomalous precession velocity ω_a:

$$\vec{\omega}_a = \vec{\omega}_s - \vec{\omega}_c = g\frac{e\vec{B}}{2m} - \frac{e\vec{B}}{m} = \left(\frac{g-2}{2}\right)\cdot\frac{e\vec{B}}{m} = a_\mu\frac{e\vec{B}}{m}$$

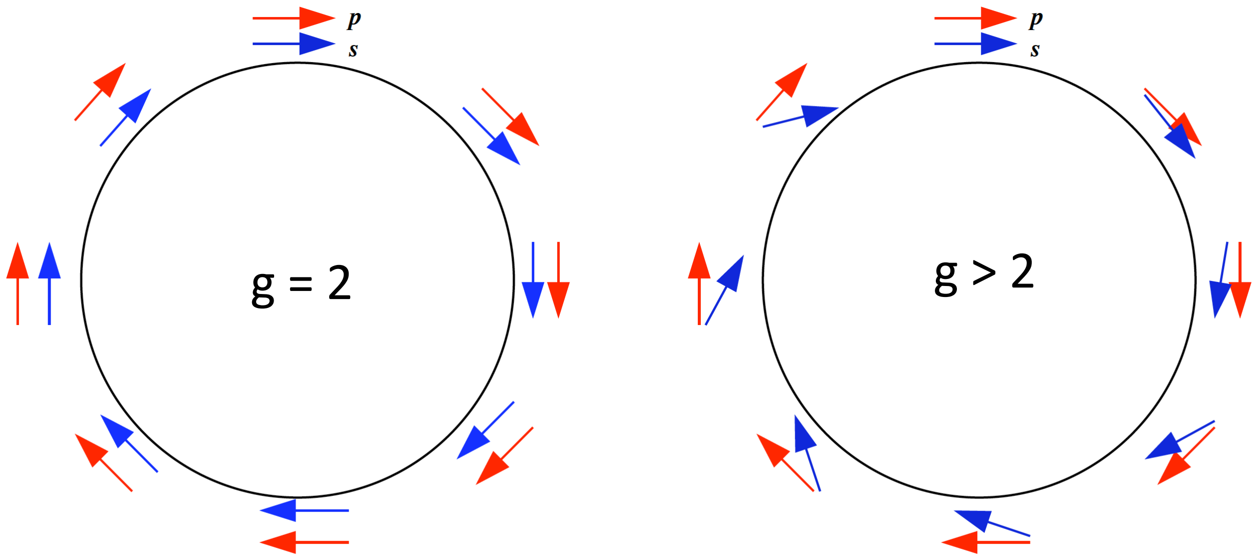

How such precision is possible?

- **4 nature gifts** allow to reach this very high precision:

How such precision is possible?

- **4 nature gifts** allow to reach this very high precision:

  1. ***Muons strongly polarized (95%):***

     - It is possible thanks to the weak pion decay

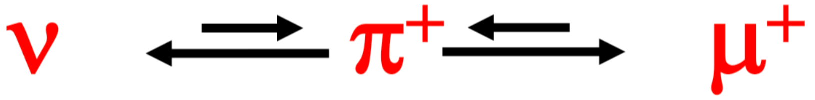

How such precision is possible?

- **4 nature gifts** allow to reach this very high precision:

1. ***Muons strongly polarized (95%):***

   - It is possible thanks to the weak pion decay

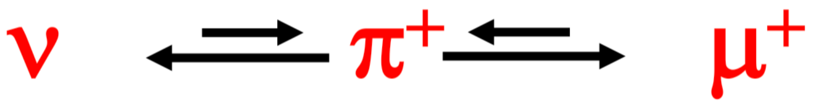

2. ***Precession frequency proportional to (g-2)***

   - $\vec{\omega}_a = \vec{\omega}_S - \vec{\omega}_c = \left(\frac{g-2}{2}\right) \cdot \frac{e\vec{B}}{m}$

How such precision is possible?

- **4 nature gifts** allow to reach this very high precision:

1. ***Muons strongly polarized (95%):***
   - It is possible thanks to the weak pion decay

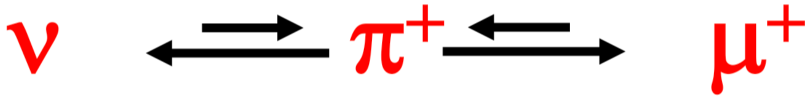

2. ***Precession frequency proportional to (g-2)***
   - $$\vec{\omega}_a = \vec{\omega}_S - \vec{\omega}_c = \left(\frac{g-2}{2}\right) \cdot \frac{e\vec{B}}{m}$$

3. ***Magic momentum*** $P_\mu = 3.094$ ***Gev/c:***
   - $$\vec{\omega}_a = \frac{e}{m}\left[a_\mu \vec{B} - \left(a_\mu - \frac{1}{\gamma^2 - 1}\right)\left(\vec{\beta} \times \vec{E}\right)\right]$$

How such precision is possible?

- **4 nature gifts** allow to reach this very high precision:

1. ***Muons strongly polarized (95%):***
   - It is possible thanks to the weak pion decay

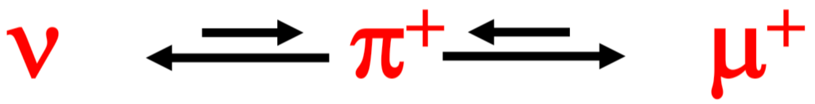

2. ***Precession frequency proportional to (g-2)***
   - $\vec{\boldsymbol{\omega}}_a = \vec{\boldsymbol{\omega}}_S - \vec{\boldsymbol{\omega}}_c = \left(\frac{g-2}{2}\right) \cdot \frac{e\vec{B}}{m}$

3. ***Magic momentum $P_\mu = 3.094$ Gev/c:*** $\gamma = \sqrt{1 + \frac{1}{a_\mu}} \sim 29.3$
   - $\vec{\omega}_a = \frac{e}{m}\left[a_\mu \vec{B} - \left(a_\mu - \frac{1}{\gamma^2 - 1}\right)\left(\vec{\beta} \times \vec{E}\right)\right]$

How such precision is possible?

- **4 nature gifts** allow to reach this very high precision:

1. ***Muons strongly polarized (95%):***
   - It is possible thanks to the weak pion decay

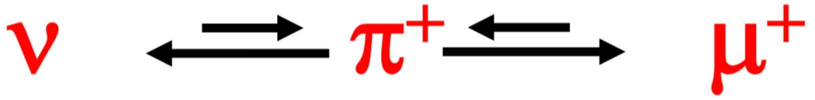

2. ***Precession frequency proportional to (g-2)***
   - $\vec{\omega}_a = \vec{\omega}_S - \vec{\omega}_c = \left(\frac{g-2}{2}\right) \cdot \frac{e\vec{B}}{m}$

3. ***Magic momentum $P_\mu = 3.094$ Gev/c:*** $\gamma = \sqrt{1 + \frac{1}{a_\mu}} \sim 29.3$
   - $\vec{\omega}_a = \frac{e}{m}\left[a_\mu \vec{B} - \left(a_\mu - \frac{1}{\gamma^2 - 1}\right)\left(\vec{\beta} \times \vec{E}\right)\right]$

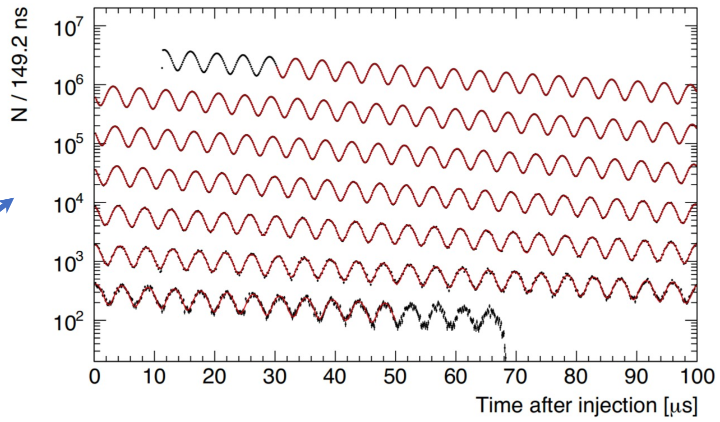

4. ***Positron emitted preferably in direction of the muon spin***

a_μ Extraction (simplified)

- The magnetic anomaly $\boldsymbol{a_\mu}$ is obtained by measuring many quantities:

$$a_\mu = \frac{\omega_a}{\tilde{\omega}'_p} \frac{\mu_p}{\mu_e} \frac{m_\mu}{m_e} \frac{g_e}{2}$$

Ratio measured at Muon g-2 experiment:

$$\boldsymbol{R' = \frac{\omega_a}{\tilde{\omega}'_p}}$$

Quantities measured in other experiments

$\boldsymbol{\tilde{\omega}'_p}$ represents the magnetic field as proton Larmor frequency (in a water sample) weighted with the beam distribution inside the ring.

g-2 short recap: The Ring

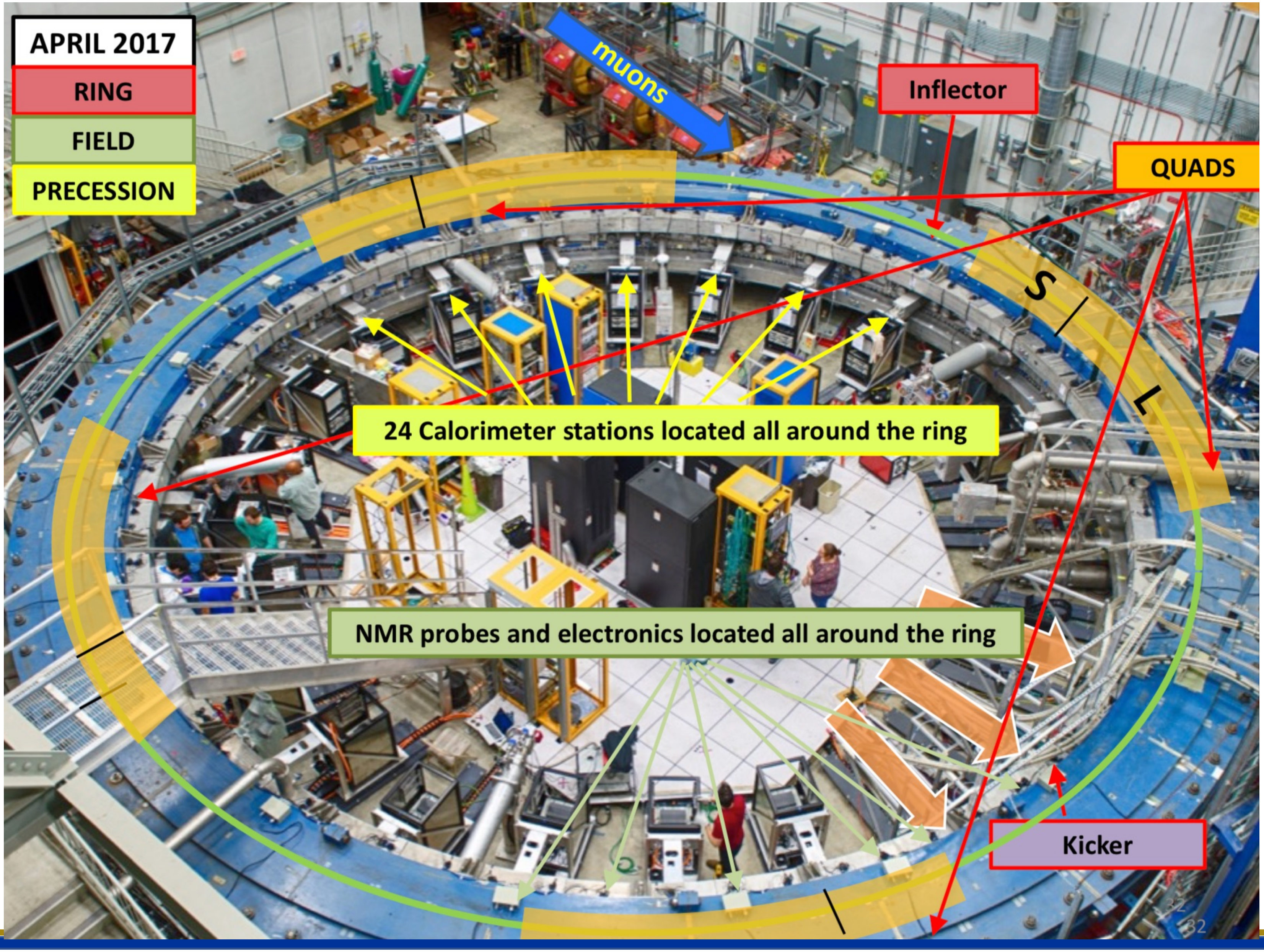

Detectors

- **24 electromagnetic calorimeters:**
  - 54 PbF2 crystals read by 54 SIPMs.
  - Crystal length 14 cm, 15 X_0.
  - Cherenkov light faster than showers (signal width ~nanoseconds).
  - **Laser calibration system**, allows the energy and time calibration of the calorimeters
- **Two straw tubes trackers.**
  - 32 planes of drift tubes filled with a 50:50 mixture of Ar/Ethane.

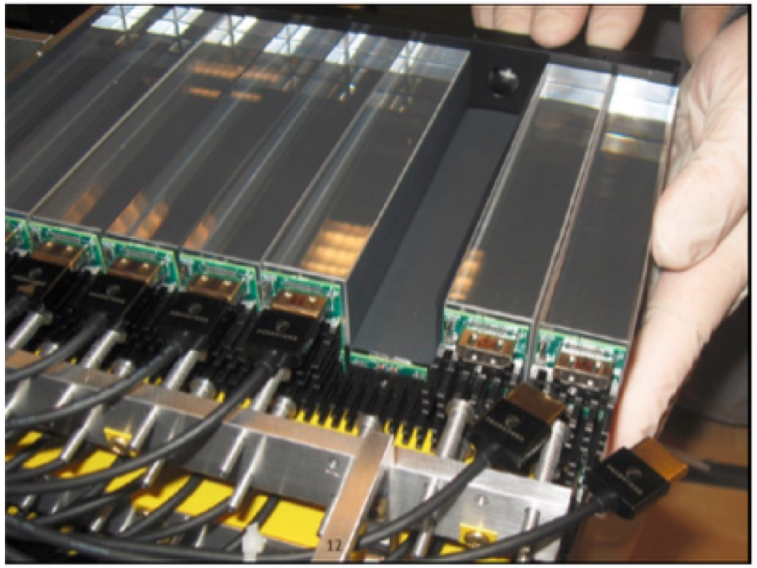

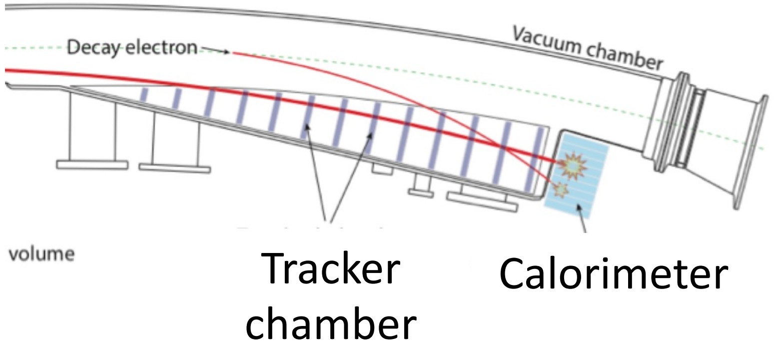

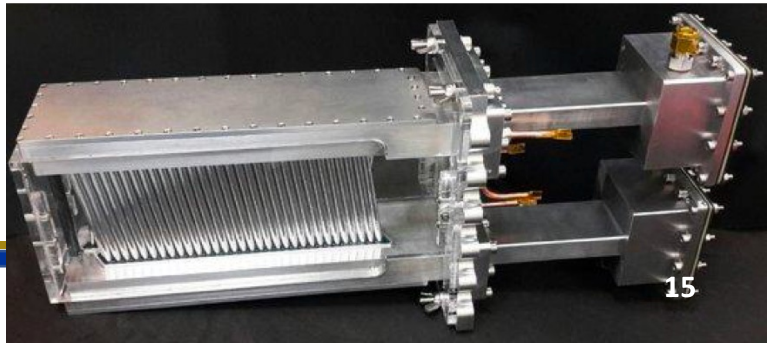

ω_a measurement

- The simplest function which describes the number of emitted positron from muon decay (so called "**wiggle plot**") is:

$$N(t) = N_0 \cdot e^{-\frac{t}{\tau}} \cdot (1 + A \cdot \cos(\omega_a \cdot t + \varphi))$$

- The **FFT** of the fit's residual shows many frequency peaks due to **beam dynamics** effects that are not modeled by the previous function.

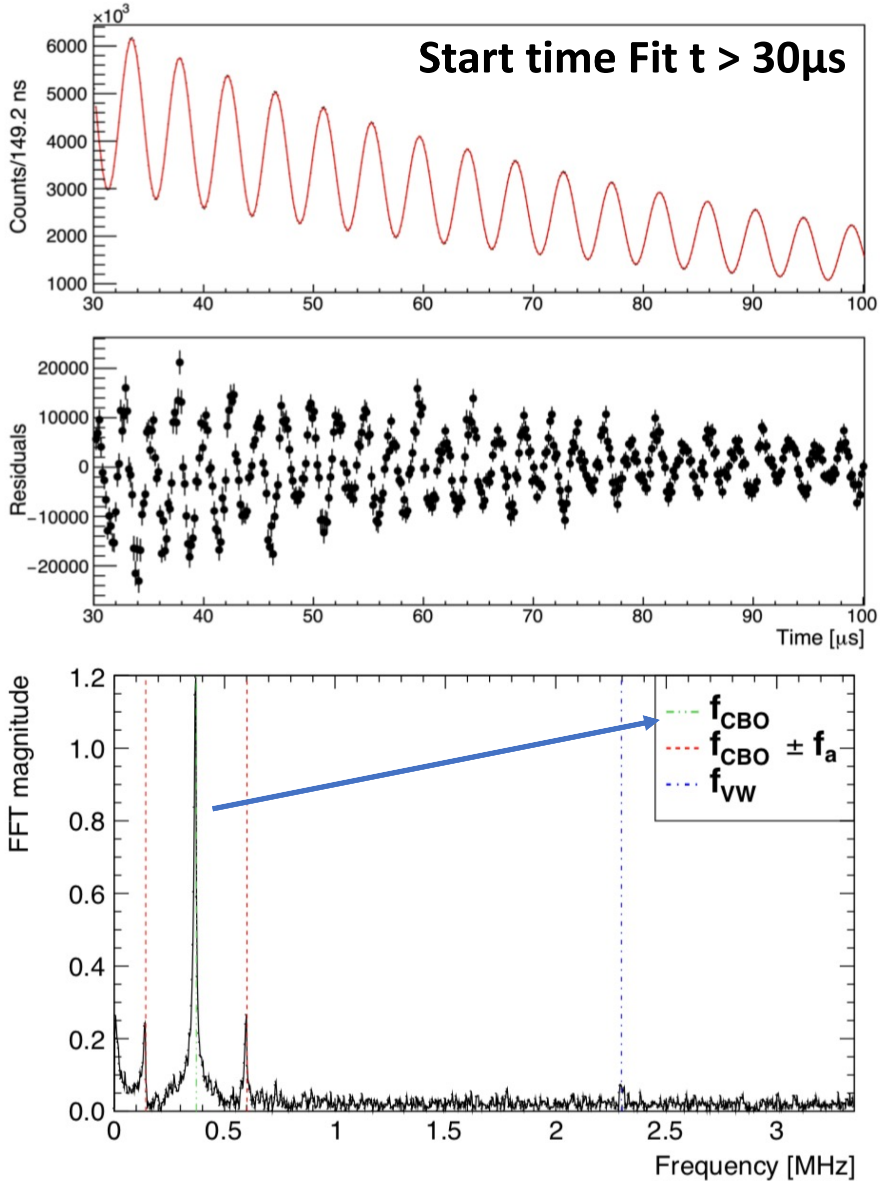

ω_a measurement

- Taking into account for the beam motion, the fit function gets more complicated up to contain up to **27 parameters**.

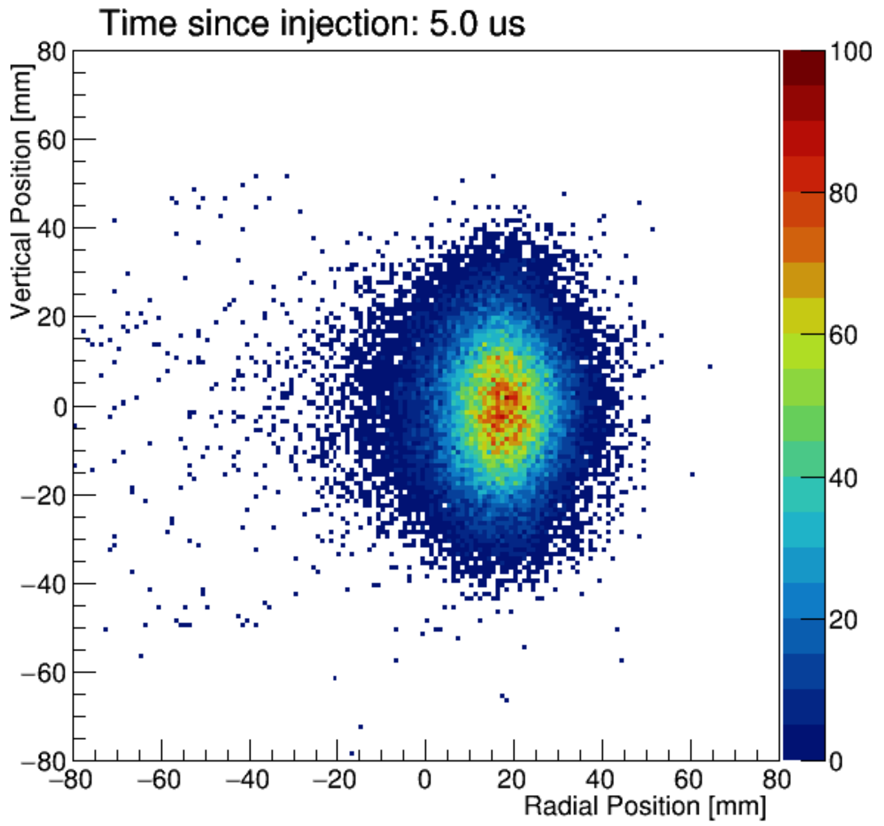

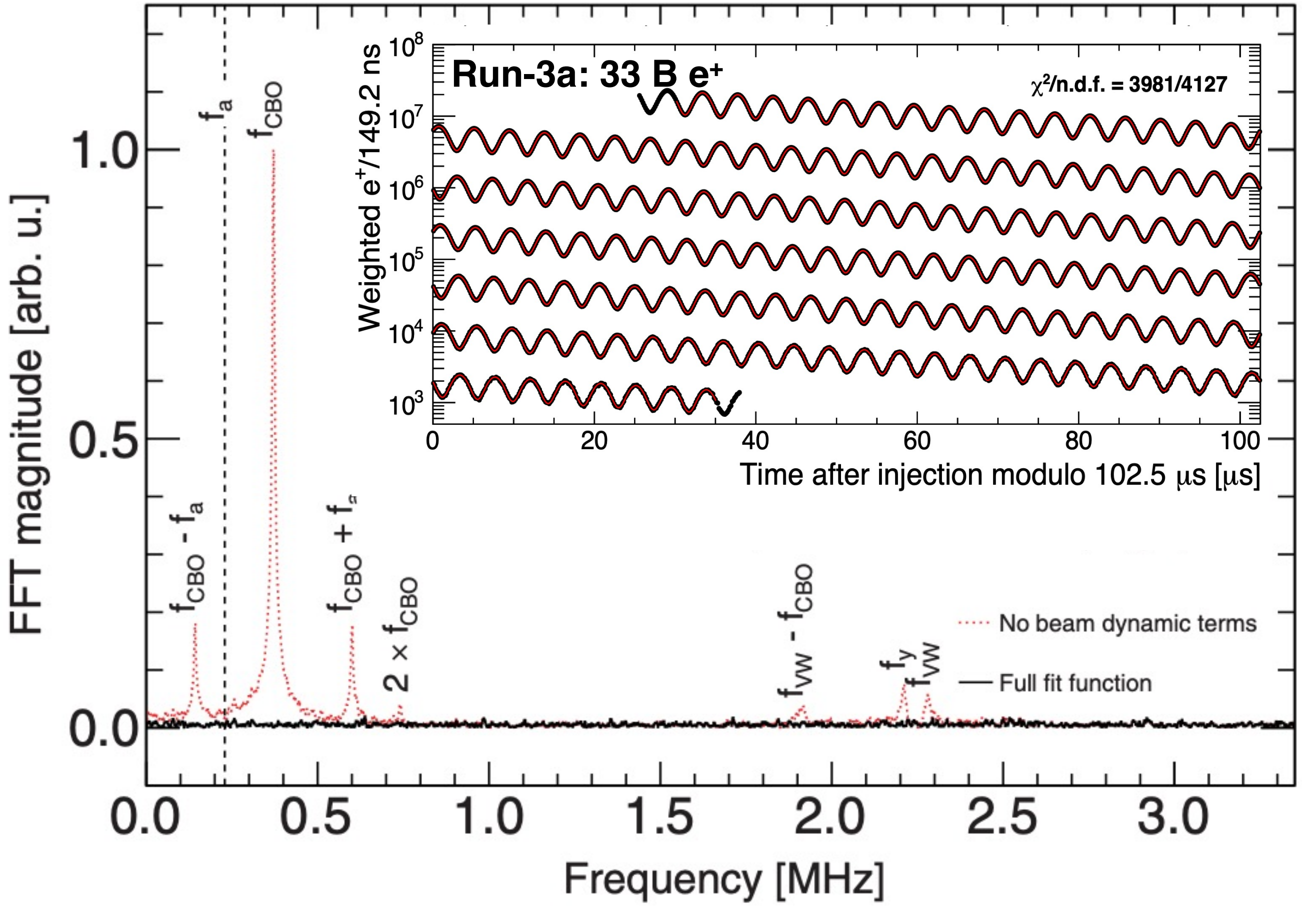

$\tilde{\omega}'_p$ Measurement

- The magnetic field is measured by:
  - **378 fixed probes** around the ring;
  - **17 NMR probes** moved around the ring via a trolley.
  - The tracker measures the muon distribution around the ring.
  - The magnetic field map is **weighted with the muon distribution** to obtain the effective field experienced by muons.

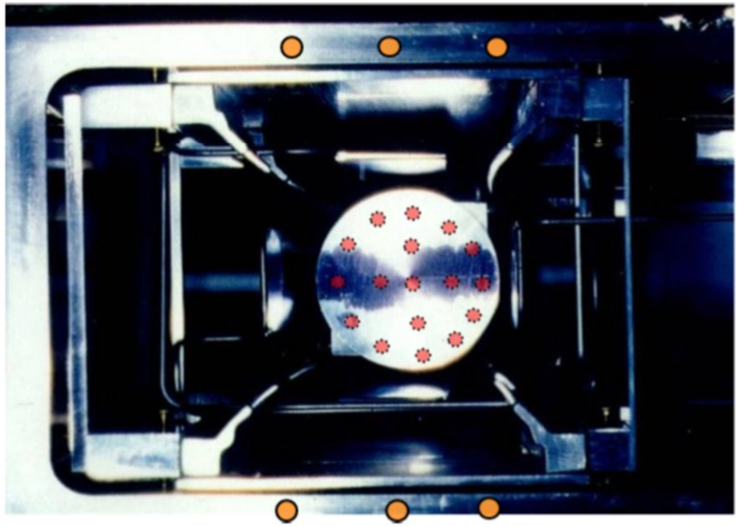

Field map

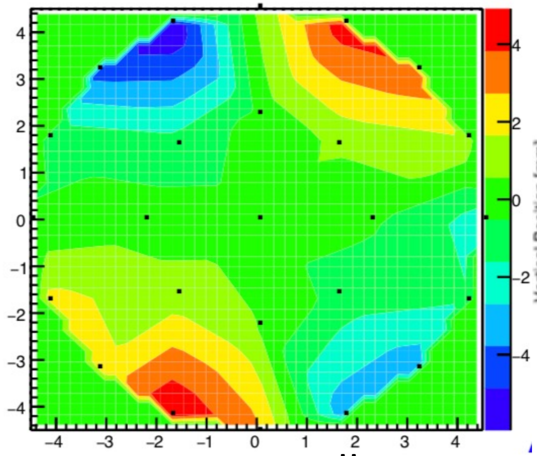

From trolley

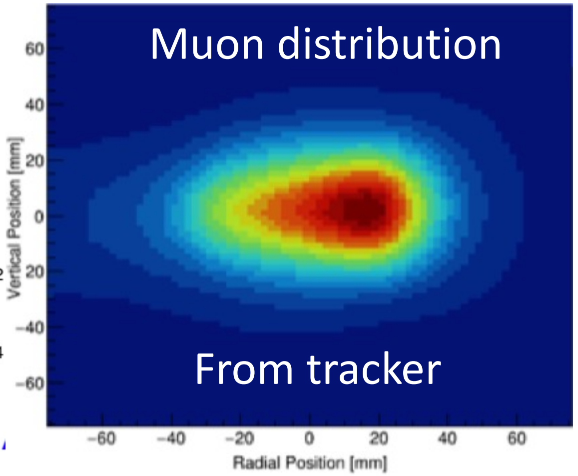

a_μ Extraction – Real world

For the measurement of a_μ the measured ω_a and ω_p need to be corrected by:

Beam dynamics corrections

$$R'_\mu \approx \frac{f_{clock}\,\omega_a^m\left(1 + C_e + C_p + C_{ml} + C_{pa} + C_{dd}\right)}{f_{calib} < \omega'_p(x,y,\phi)\times M(x,y,\phi) > \left(1 + B_k + B_q\right)}$$

Transient field corrections

The total size of the corrections in **Run-2/3** is **622 ppb** dominated by $\boldsymbol{C_e}$ and $\boldsymbol{C_p}$.
Corrections are small, but dominated Run-1 systematics…

Run-1 systematic: Where can we improve?

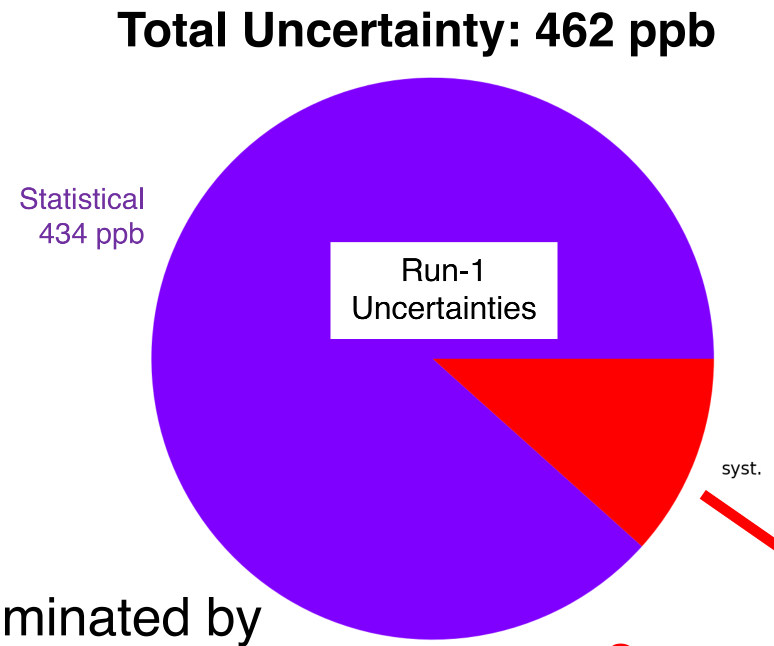

Dominated by statistical error

Systematic
157 ppb

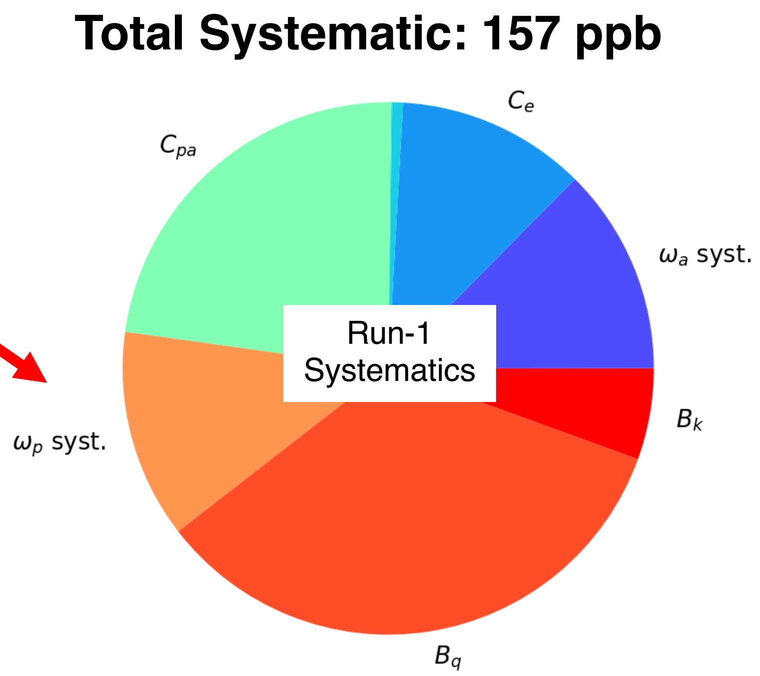

Target: quadrupole transient field B_q and phase-acceptance effect C_{pa}

Run-2/3 - Improvements

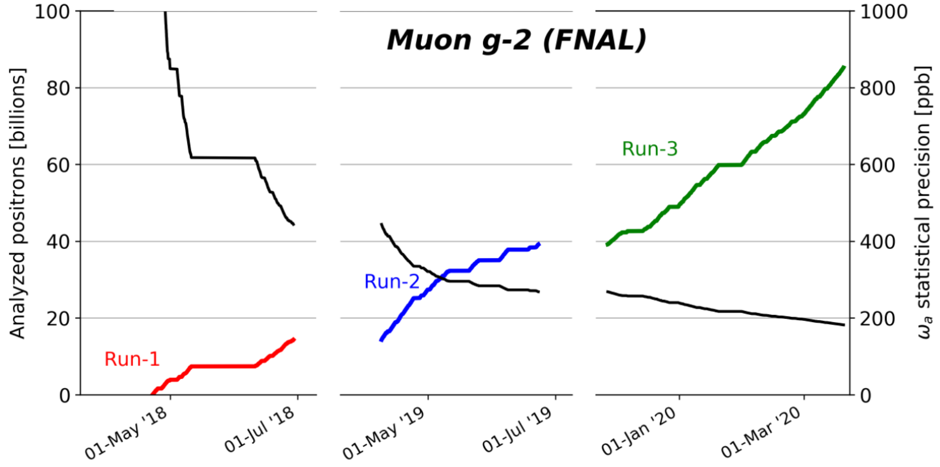

Statistics

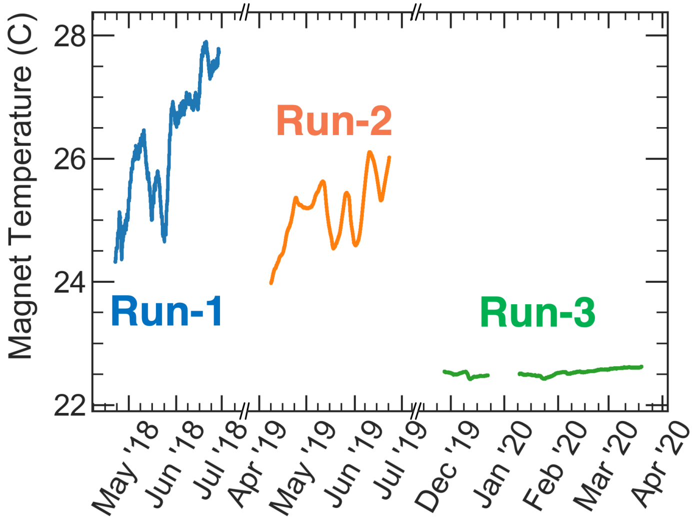

Running Conditions

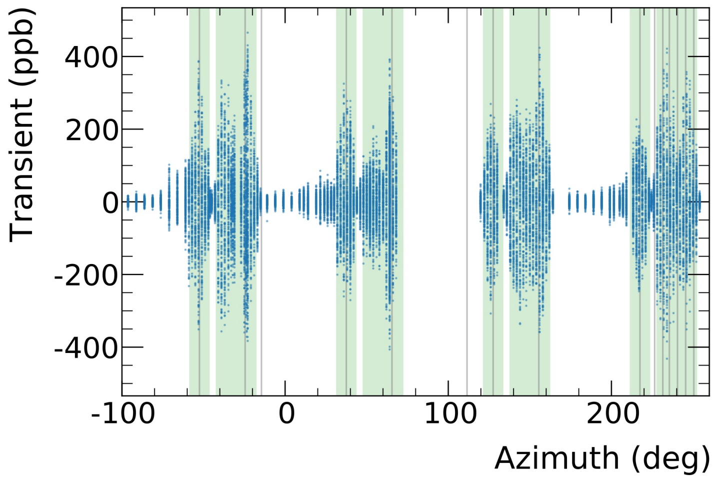

Systematic Measurements & Studies

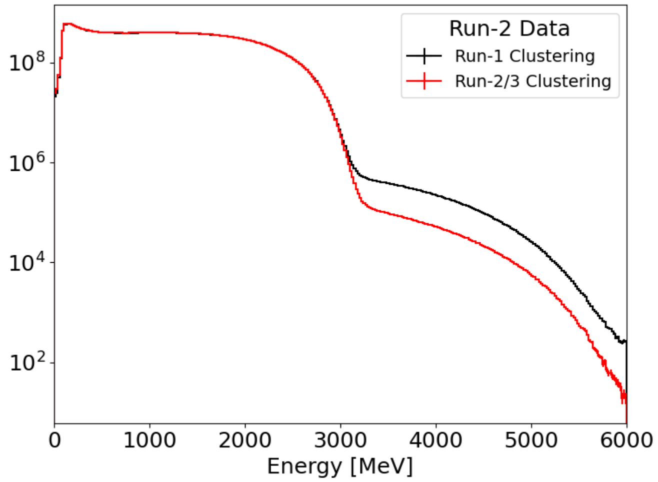

Analysis Improvements

Run-2/3 - Improvements

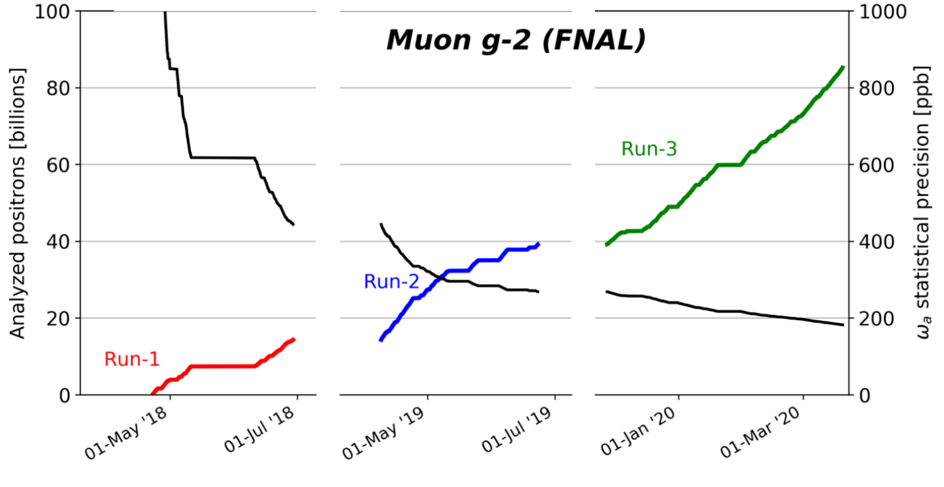

Statistics

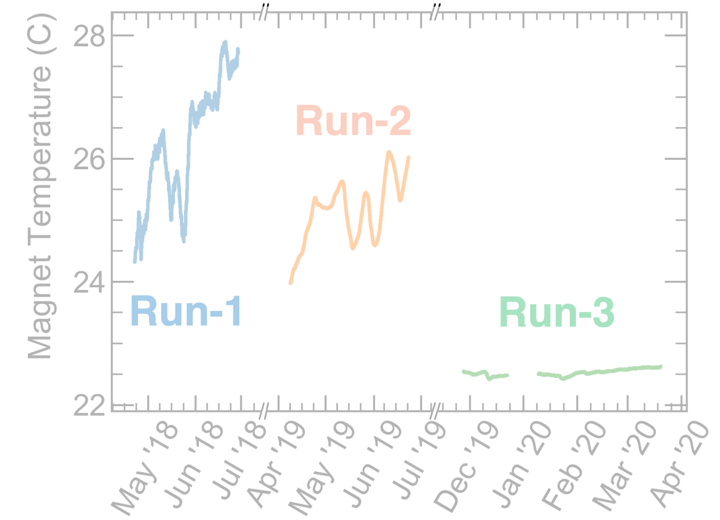

Running Conditions

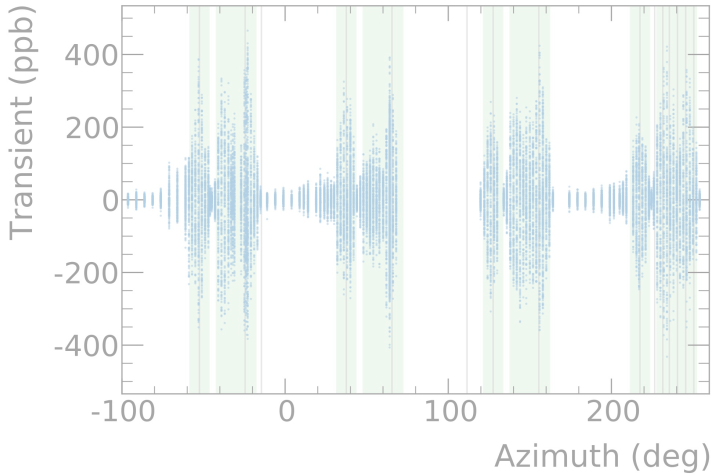

Systematic Measurements & Studies

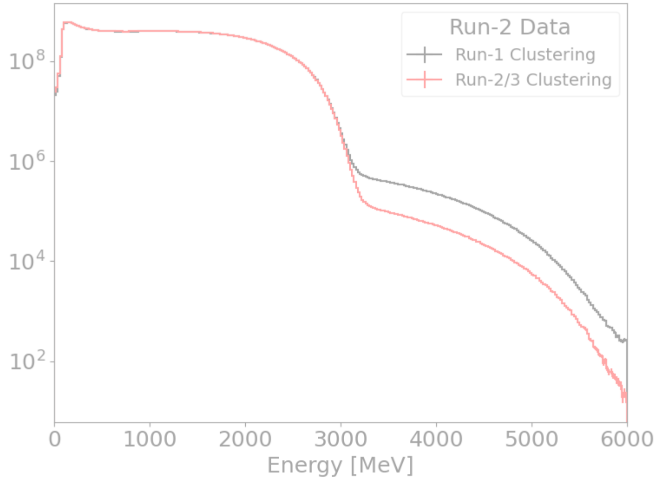

Analysis Improvements

Run-2/3 – Improvements: Statistics

Weighted e⁺ in our final fit after quality control

E > 1 GeV
t > 30 us

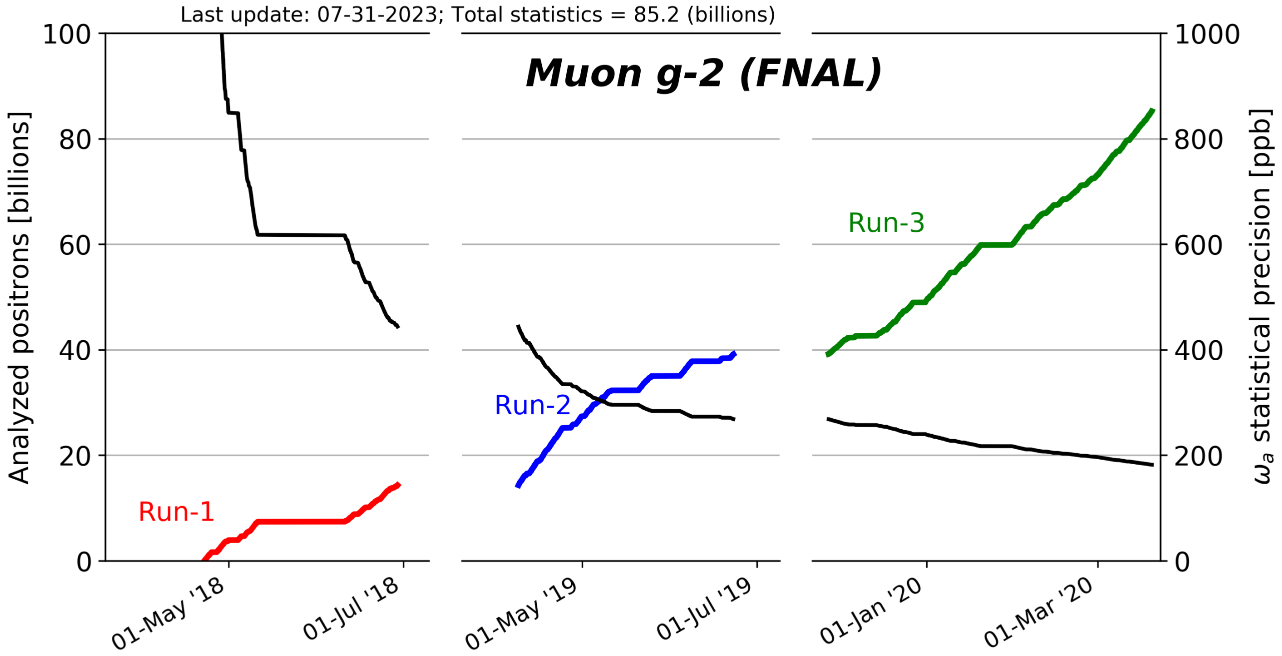

- Factor 4.7 more data in Run-2/3 than Run-1

Dataset	Statistical Error [ppb]
Run-1	434
Run-2/3	201
Run-1 + Run-2/3	185

Run-2/3 - Improvements

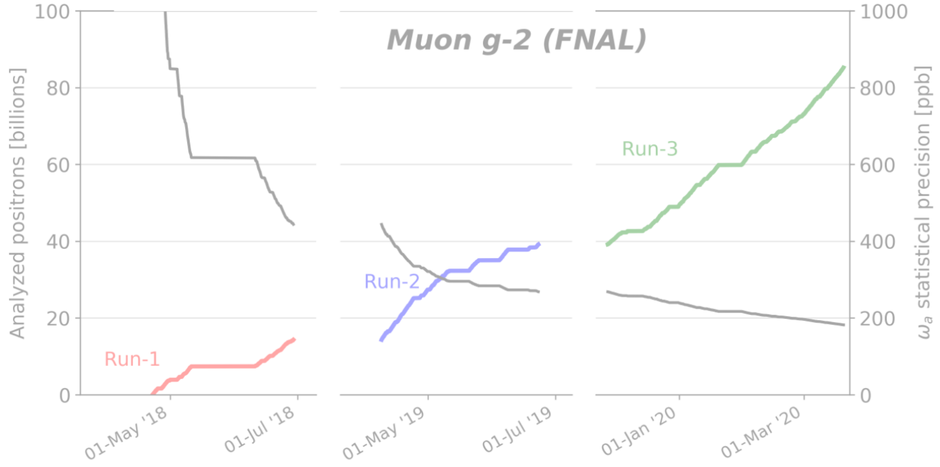

Statistics

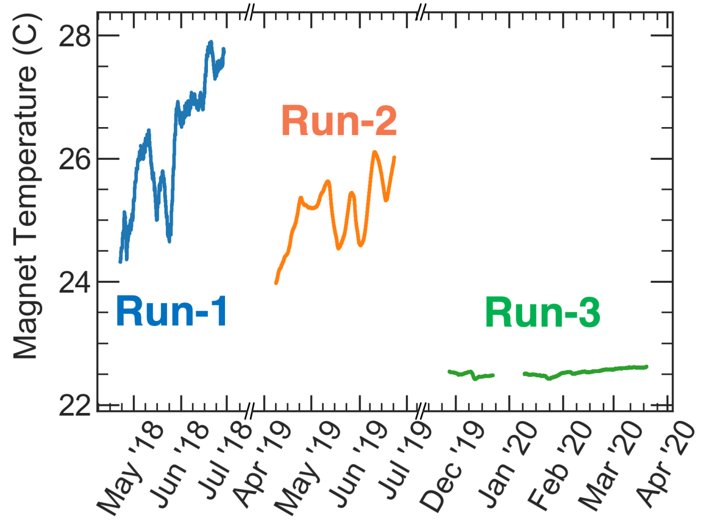

Running Conditions

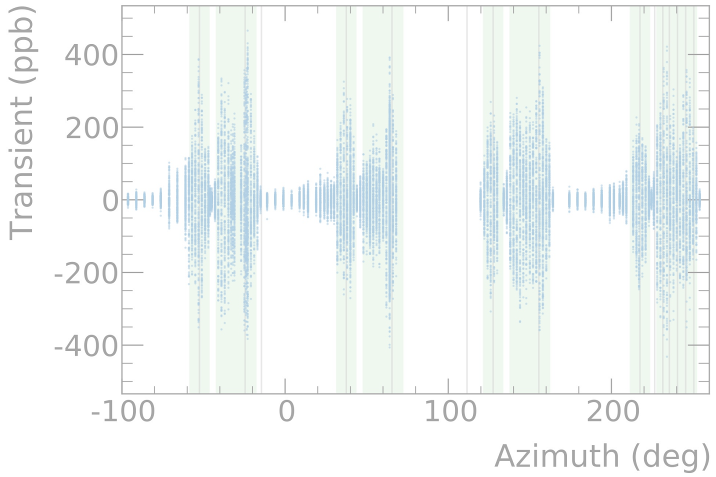

Systematic
Measurements & Studies

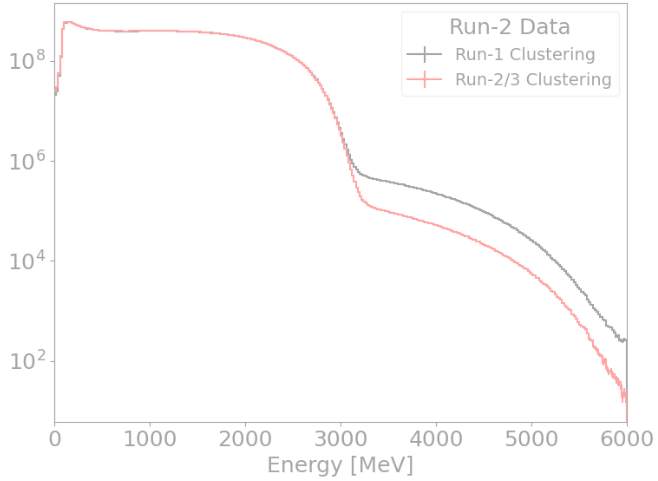

Analysis Improvements

Run-2/3 – Improvements: Running conditions

- Run-1 had **damaged resistors** in 2/32 quad plates leading to **unstable beam storage**
- Resistors re-designed & **replaced before Run-2**

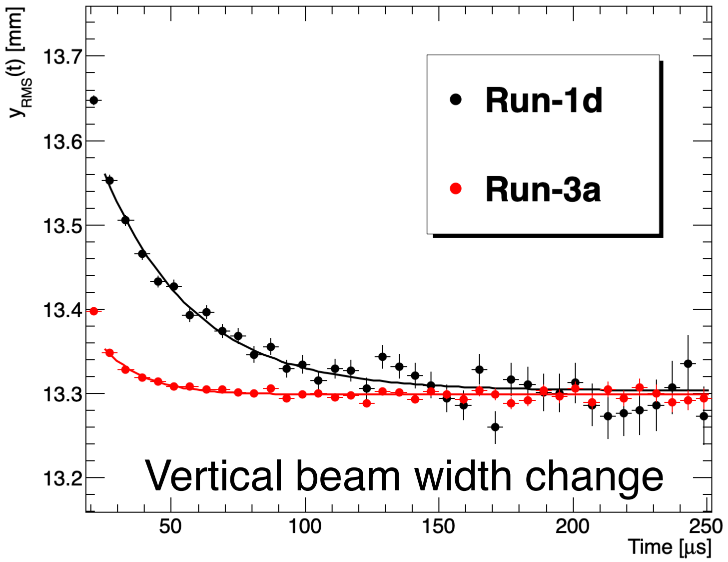

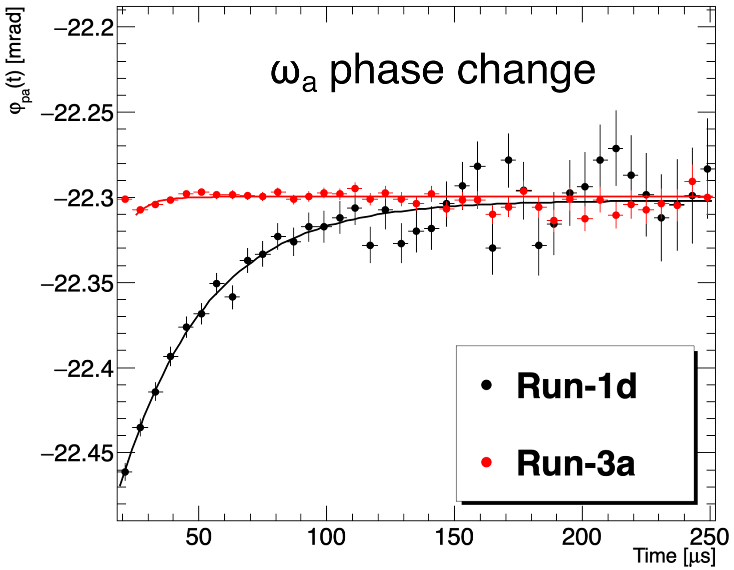

- **C_{pa}** uncertainty is reduced (**75 ppb → 13 ppb**)
- Beam **oscillation frequencies** are also **more stable**

Run-2/3 – Improvements: Running conditions

- Temperature stability makes magnetic field less variable

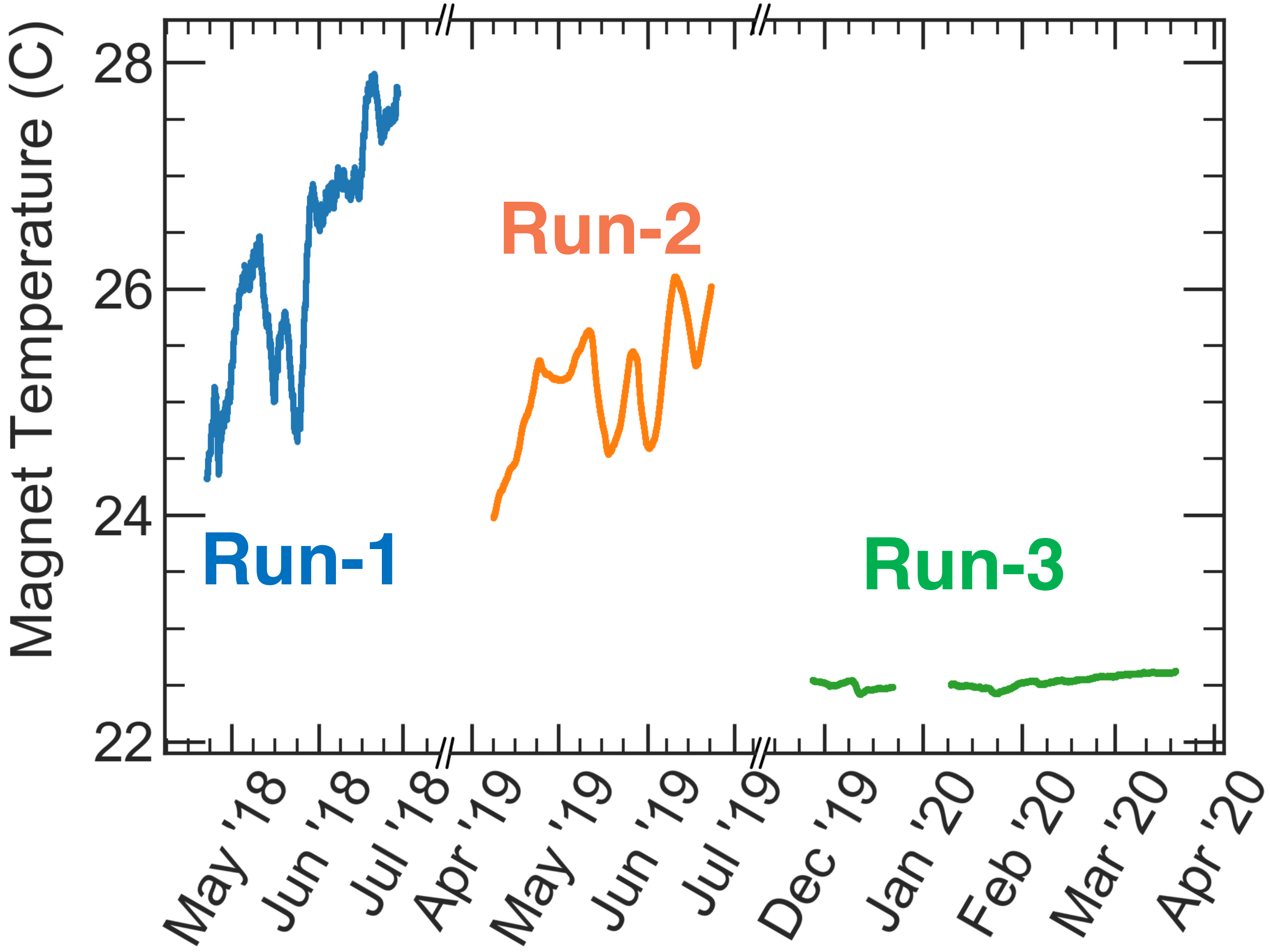

Run-2/3 – Improvements: Running conditions

- Temperature stability makes magnetic field less variable

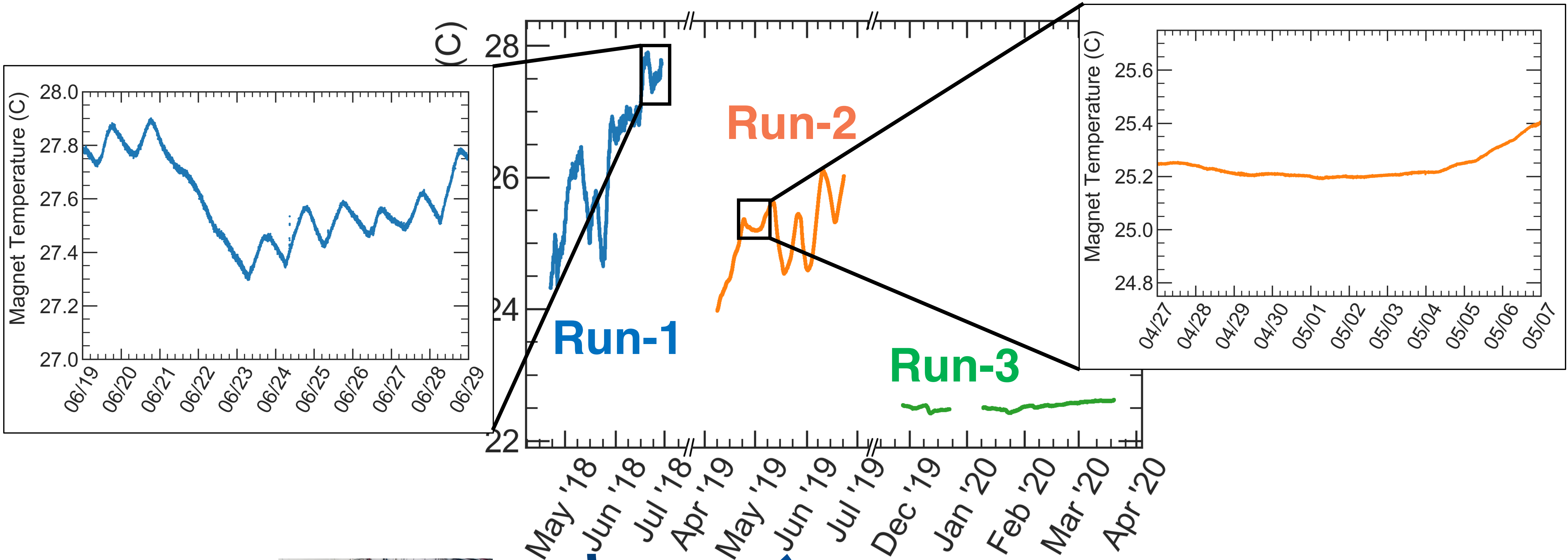

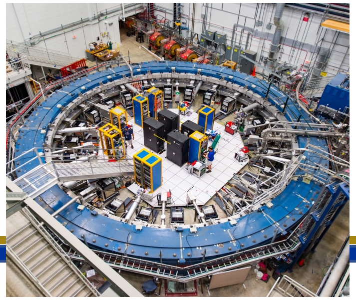

Added Insulation

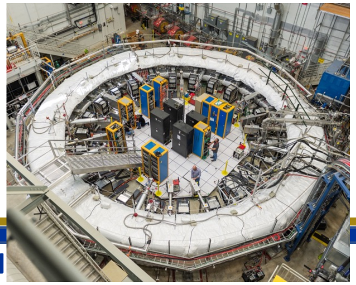

Run-2/3 – Improvements: Running conditions

- Temperature stability makes magnetic field less variable

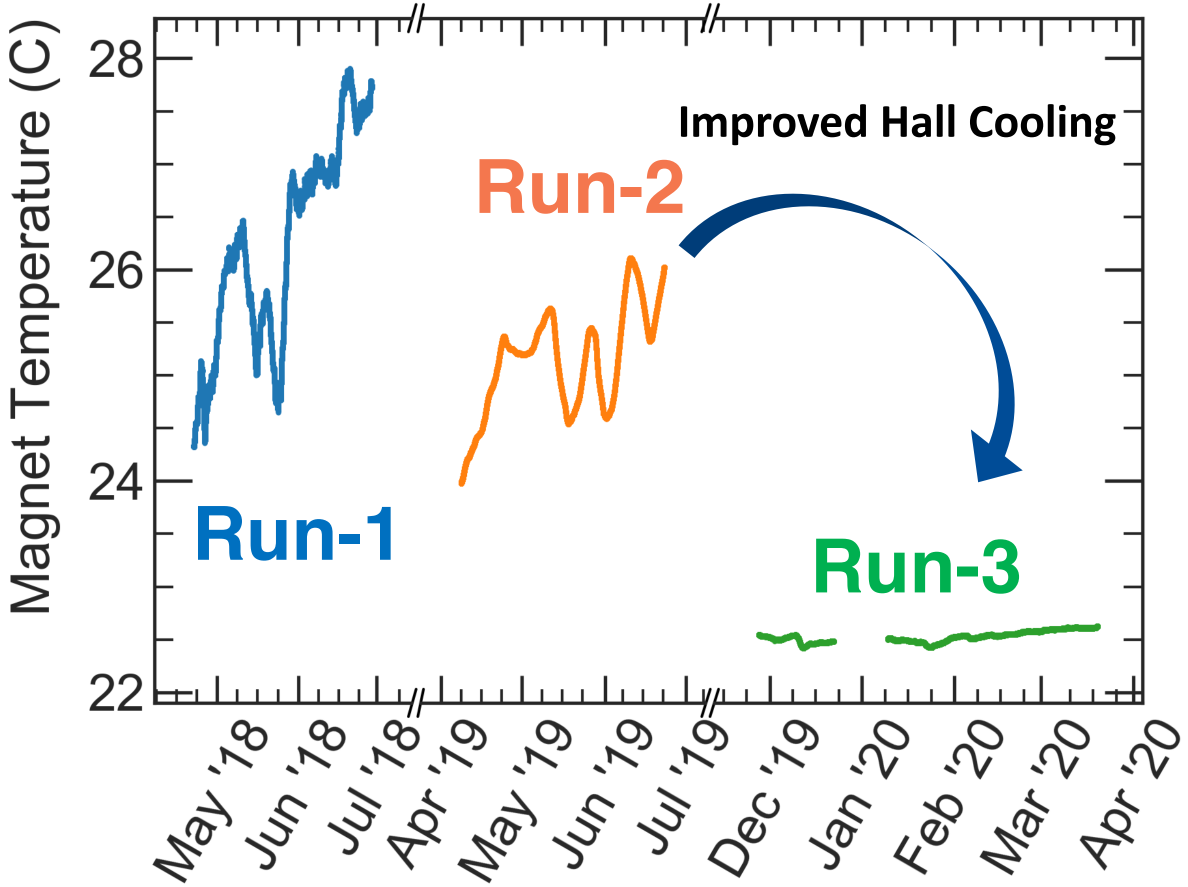

Run-2/3 – Improvements: Running conditions

- Last 18% of Run-2/3 has **upgraded, stronger kicker**

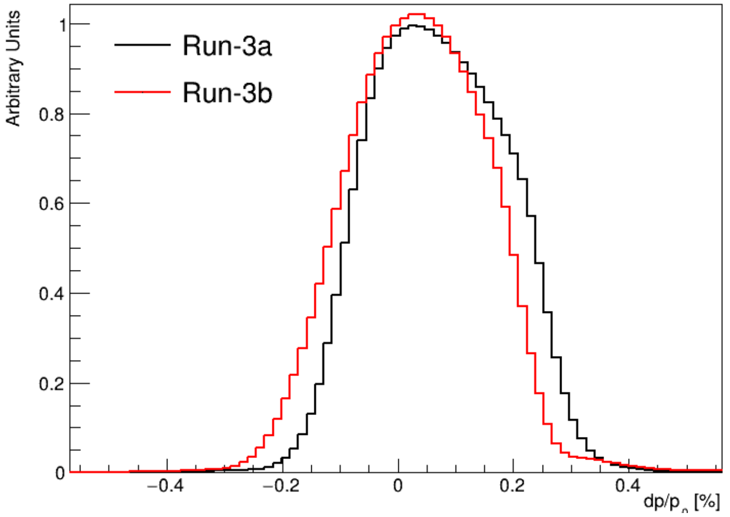

Fractional Momentum Shift: dp/p0 [%]

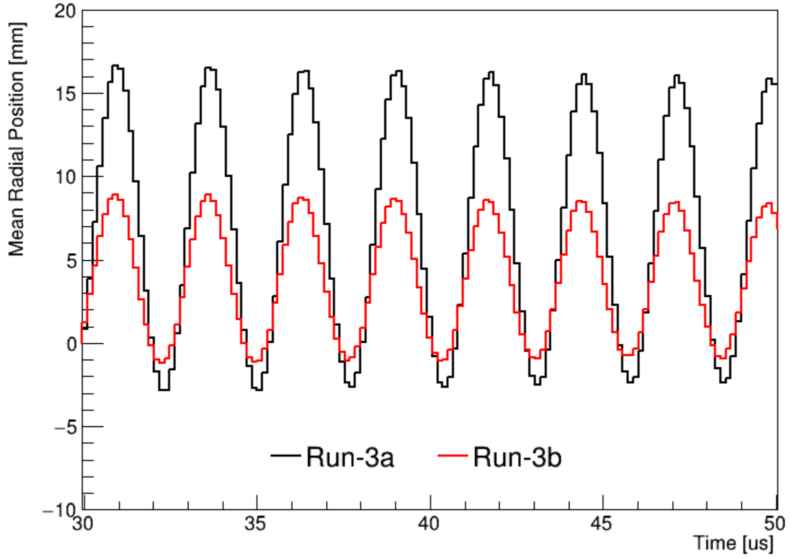

- Momentum distribution more centered
- **Lower E-field correction C_e**

- Phase space matching improved
- **Smaller beam oscillations**

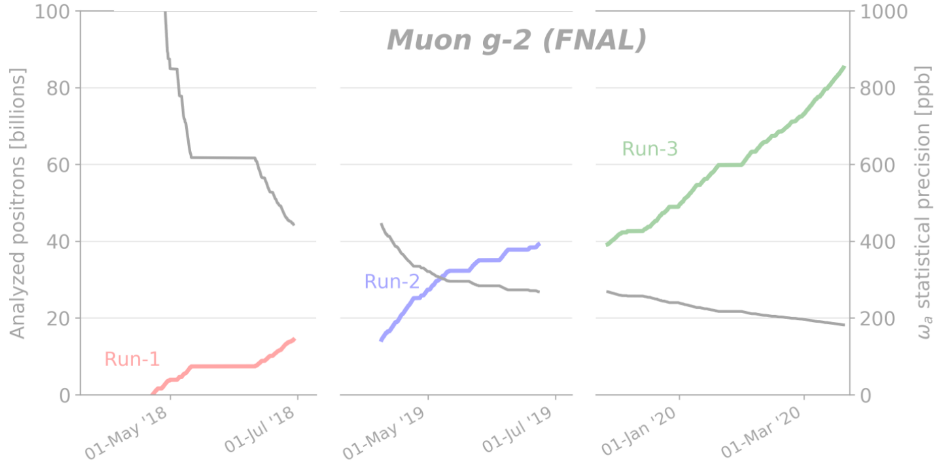

Statistics

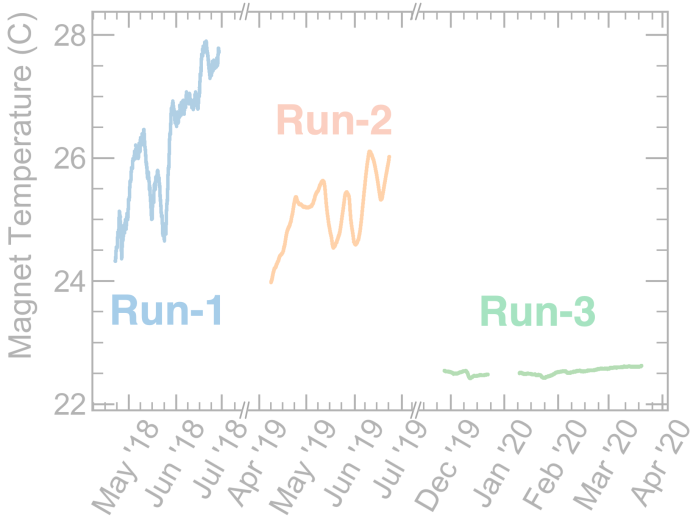

Running Conditions

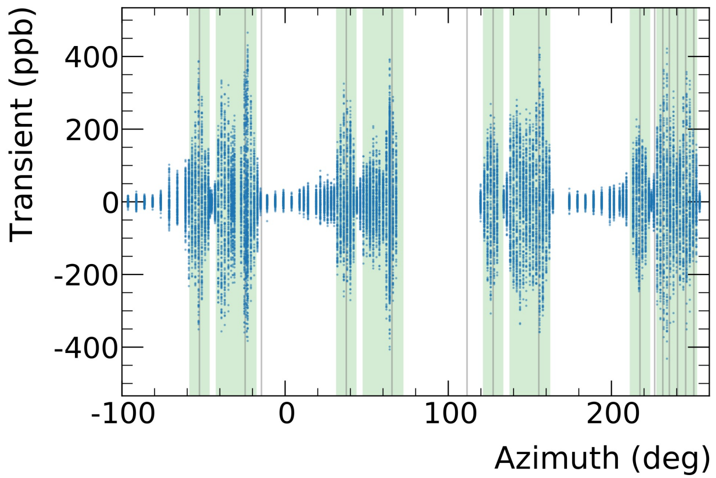

Systematic Measurements & Studies

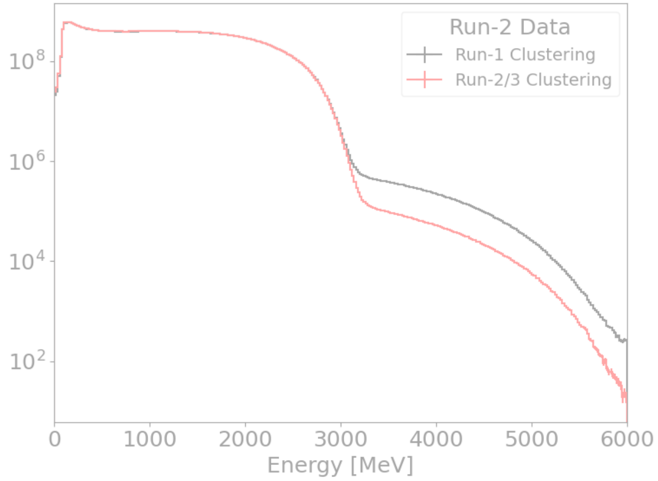

Analysis Improvements

Run-2/3 – Improvements: Improved measuremenet

- Pulsing **quads vibrate → oscillating magnetic field**
- Measured with a **new NMR probe**

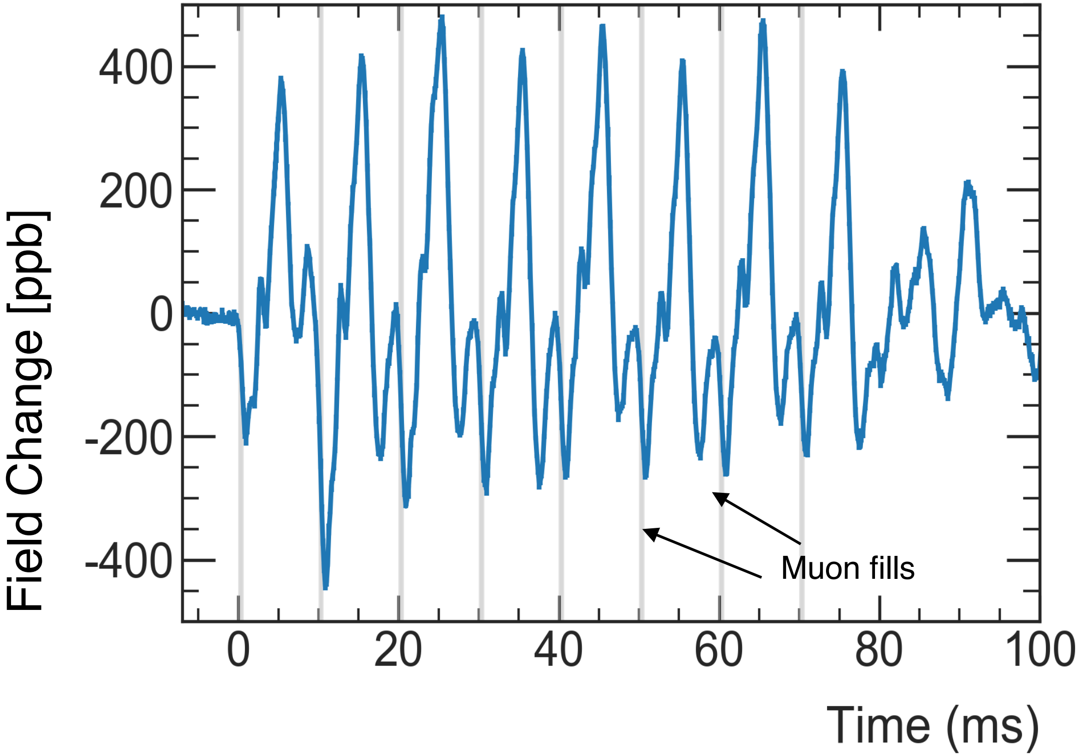

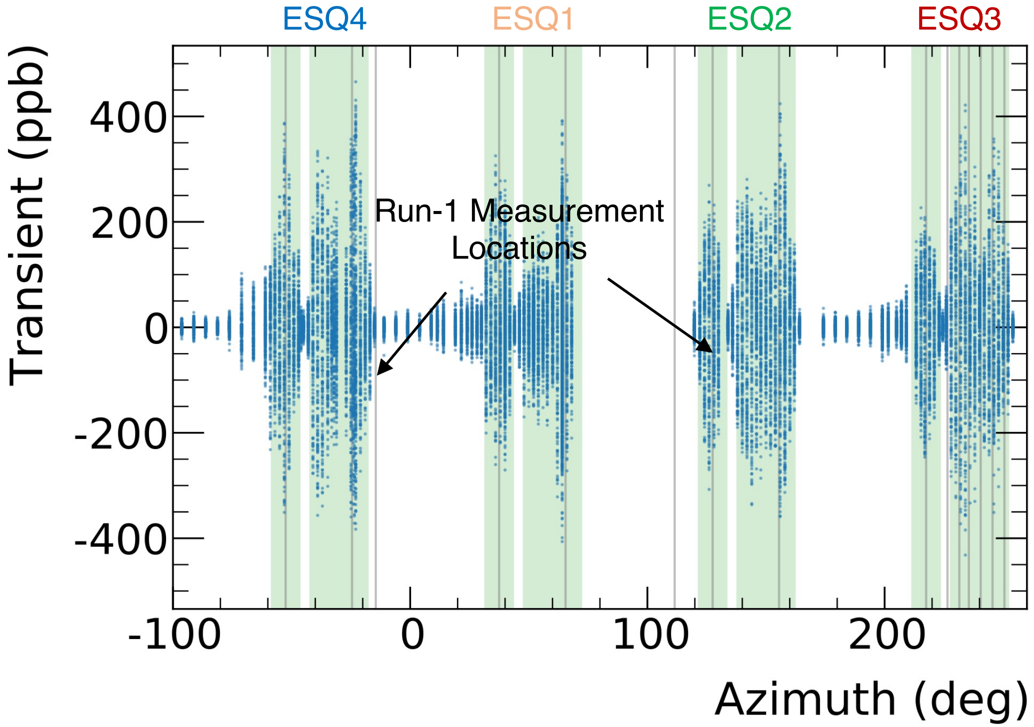

For Run-1 analysis, we had **limited measurement positions**

Largest Run-1 systematic: **92 ppb** reduced to **20 ppb**

Run-2/3 – Improvements: Improved measuremenet

- Kicker creates **eddy currents → transient magnetic field**

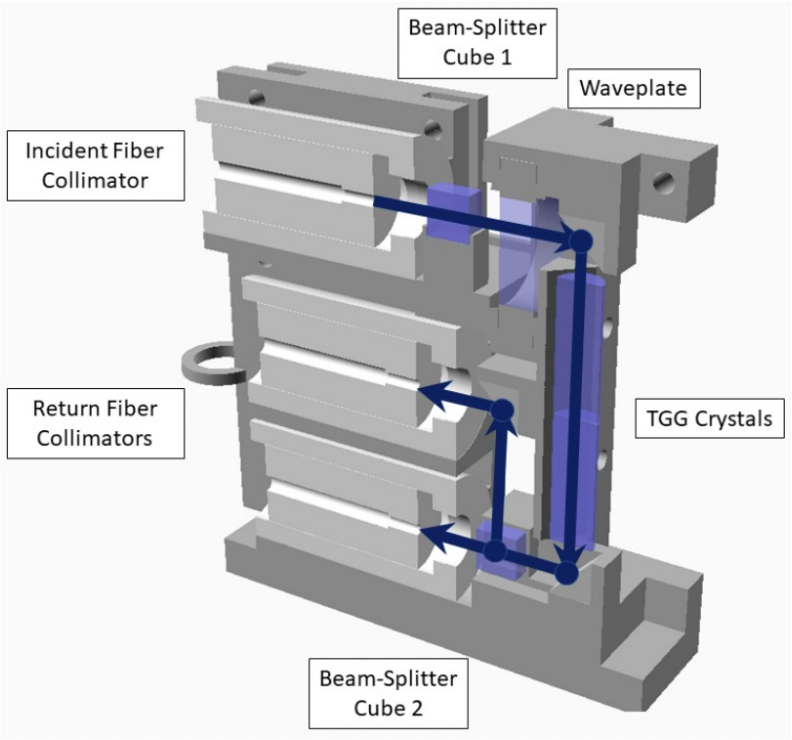

Faraday magnetometer

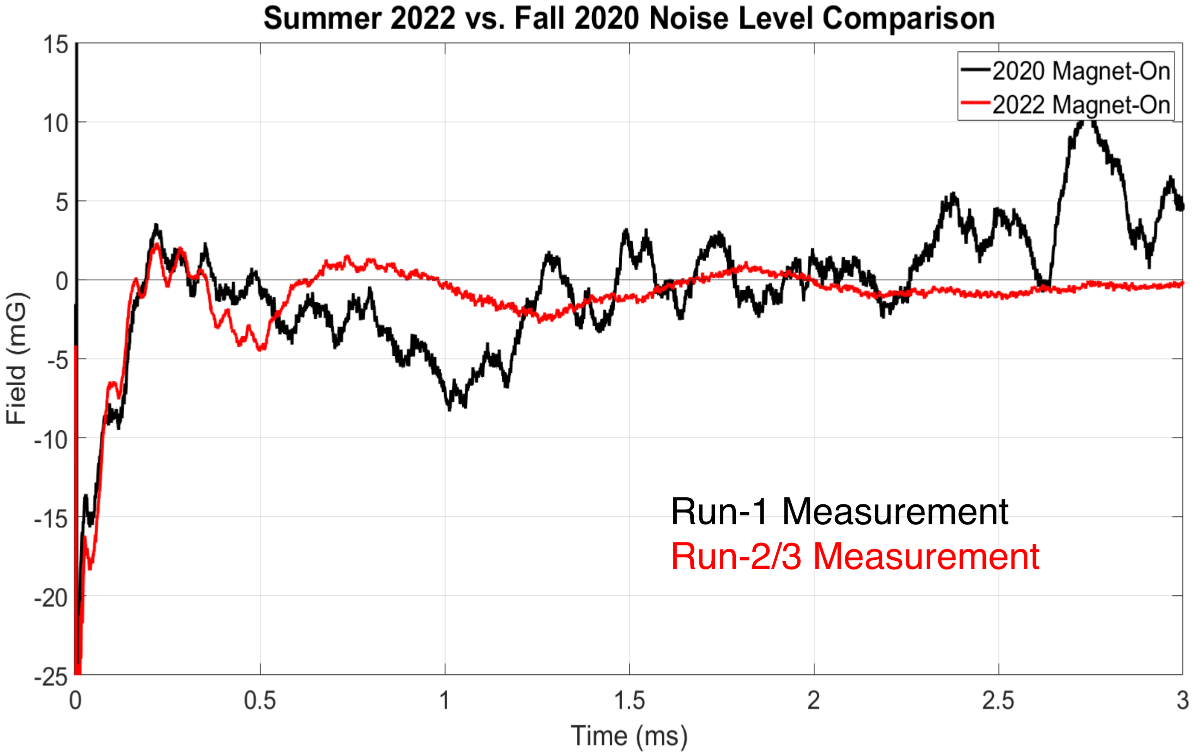

- Run-2/3 has **lower vibration noise** vs. Run-1

- Uncertainty reduced from **37 ppb** to **13 ppb**

Run-2/3 - Improvements

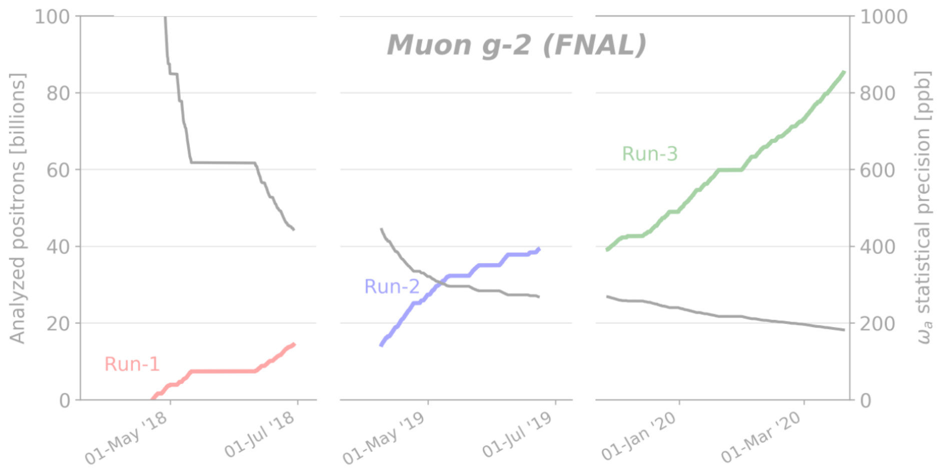

Statistics

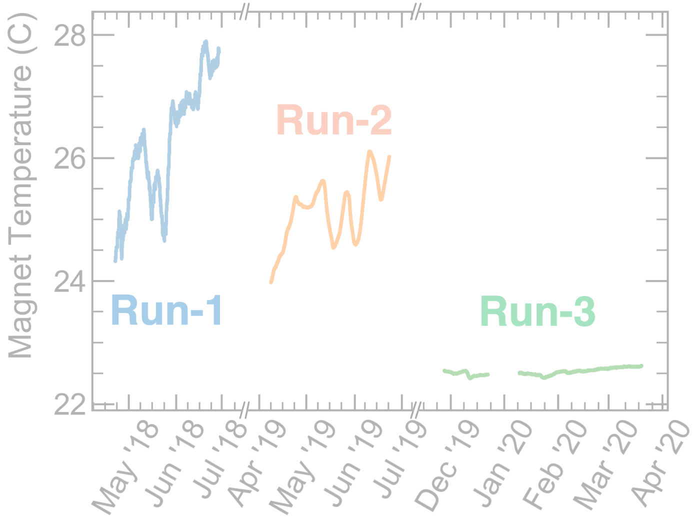

Running Conditions

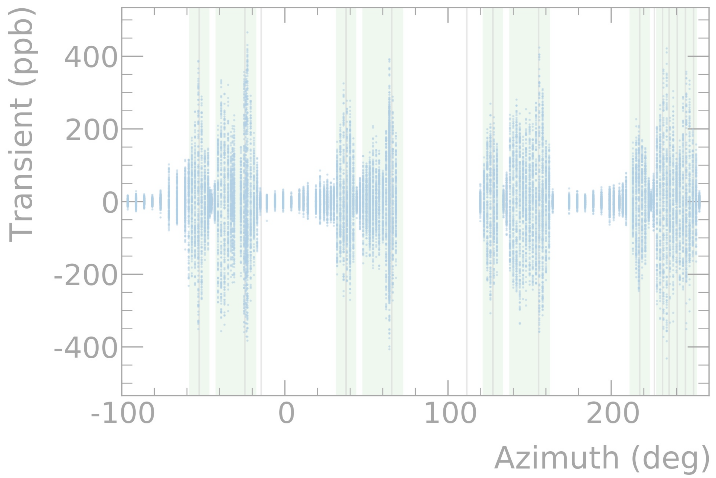

Systematic

Measurements & Studies

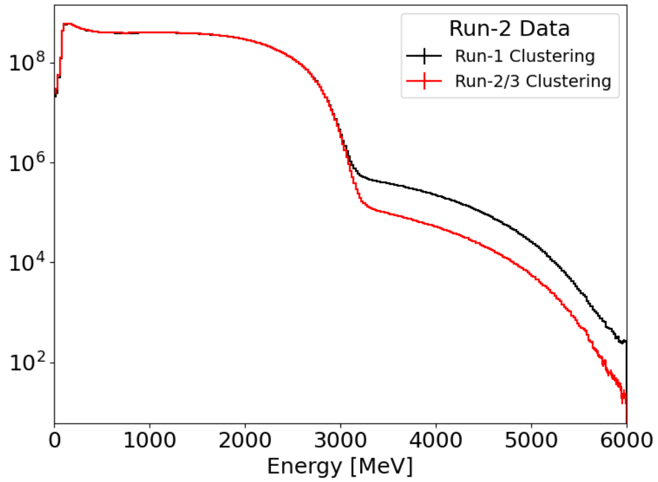

Analysis Improvements

Run-2/3 – Improvements: Analysis improvements

- 2 e^+ **arriving at same time** can be mistaken for 1: can **bias ω_a**
- Reduced uncertainty by:
  - Improved **reconstruction**
  - Improved **correction algorithms**

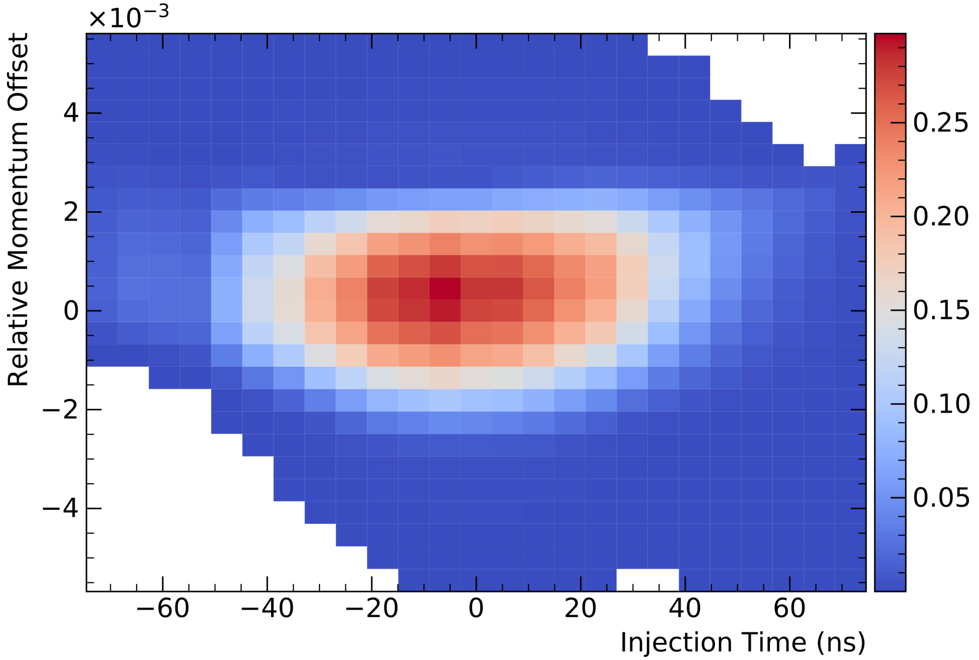

Run-1: 53 ppb to **Run-2/3:** **32 ppb**

Run-1: 35 ppb to **Run-2/3:** **7 ppb**

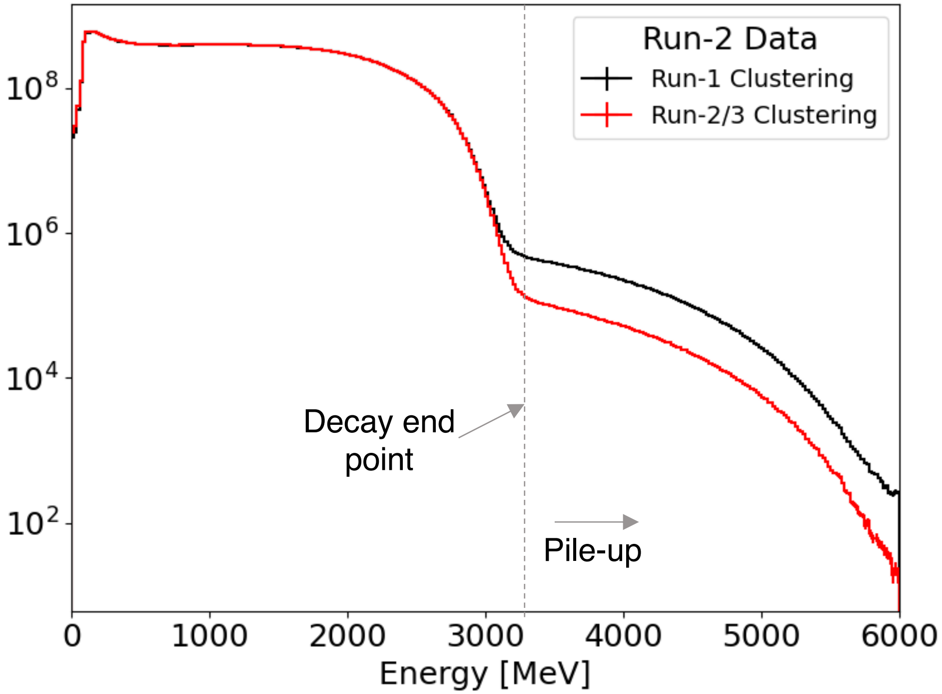

- **E-field correction** depends on **muon momentum distribution**
- Now **include correlations** between **momentum & time** of injection

Blind analysis and unblinding

- The analysis is performed with a double blinding one software and one hardware.
- Hardware blinding comes from altering our clock frequency randomly **$\pm$25ppm shift**

- On **24th July** the secret numbers have been unveiled, revealing the hidden frequency

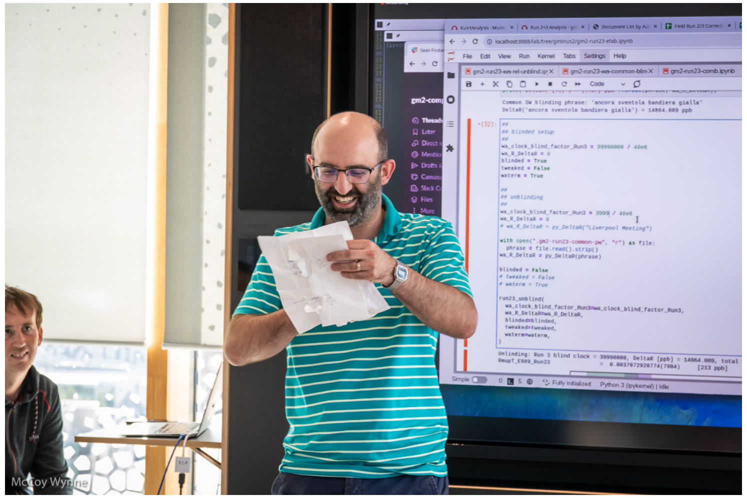

Run-2/3 Result

a_μ(FNAL) = 0.00 116 592 055(24) [203 ppb]

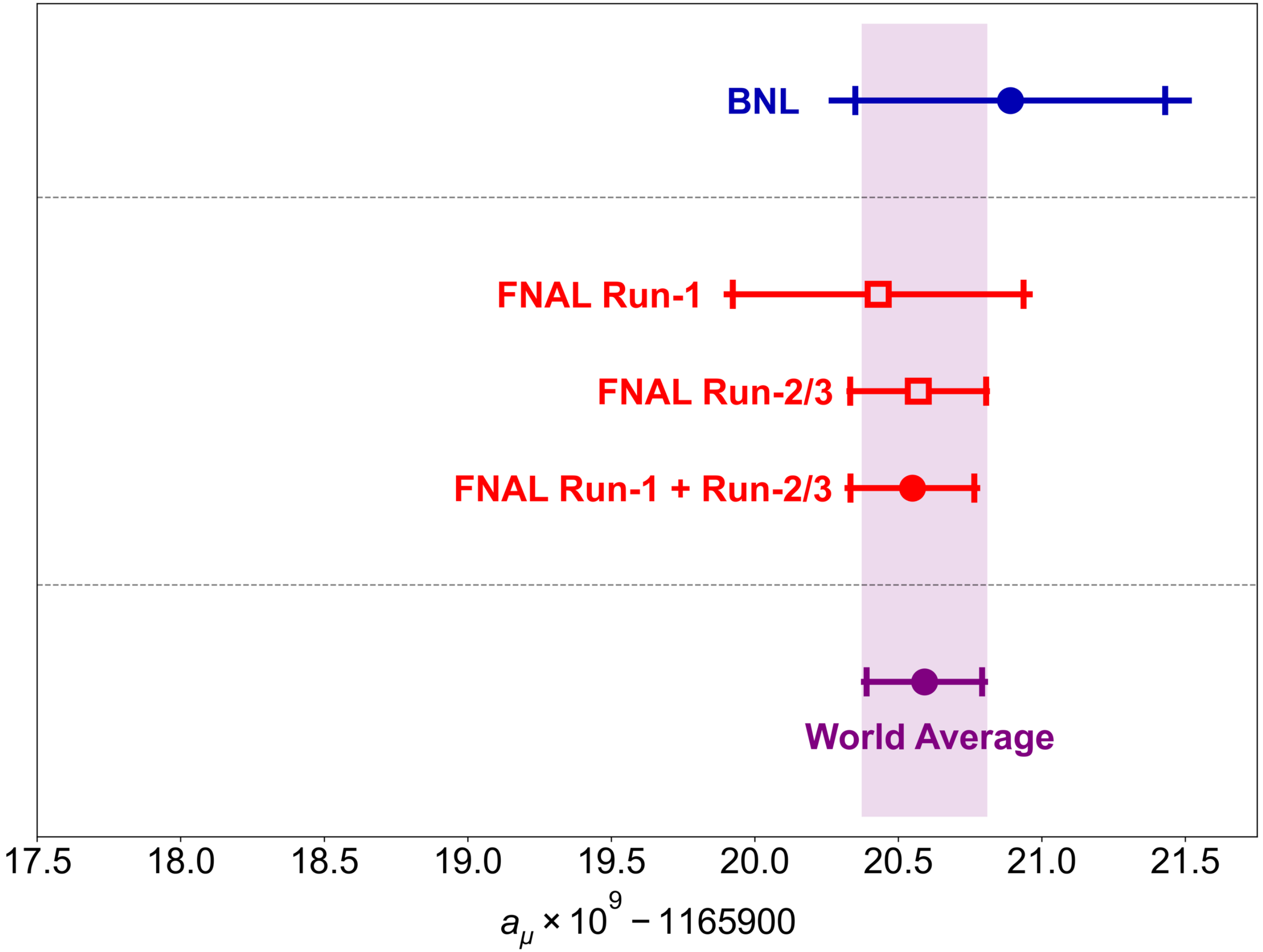

- Both FNAL and BNL dominated by statistical error
- Combined world average **dominated by FNAL** values.

a_μ(Exp) = 0.00 116 592 059(22) [190 ppb]

Run-2/3 Result

- Datasets were taken at slightly different field settings
- Allows a cross check with one of the most basic “handles”

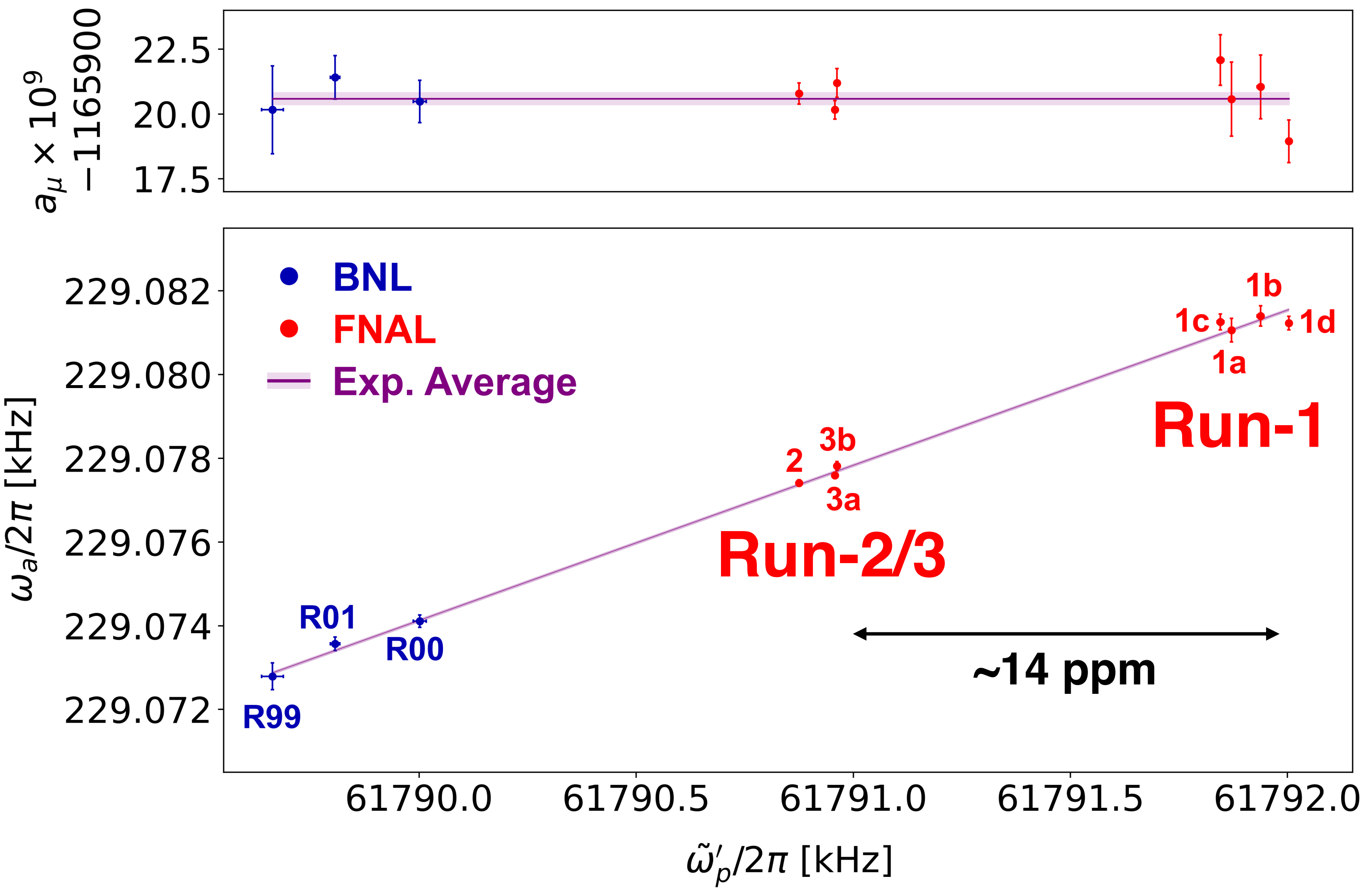

Run-2/3 Uncertainties summary

Analysis Improvements

Running Conditions

Improved Measurements

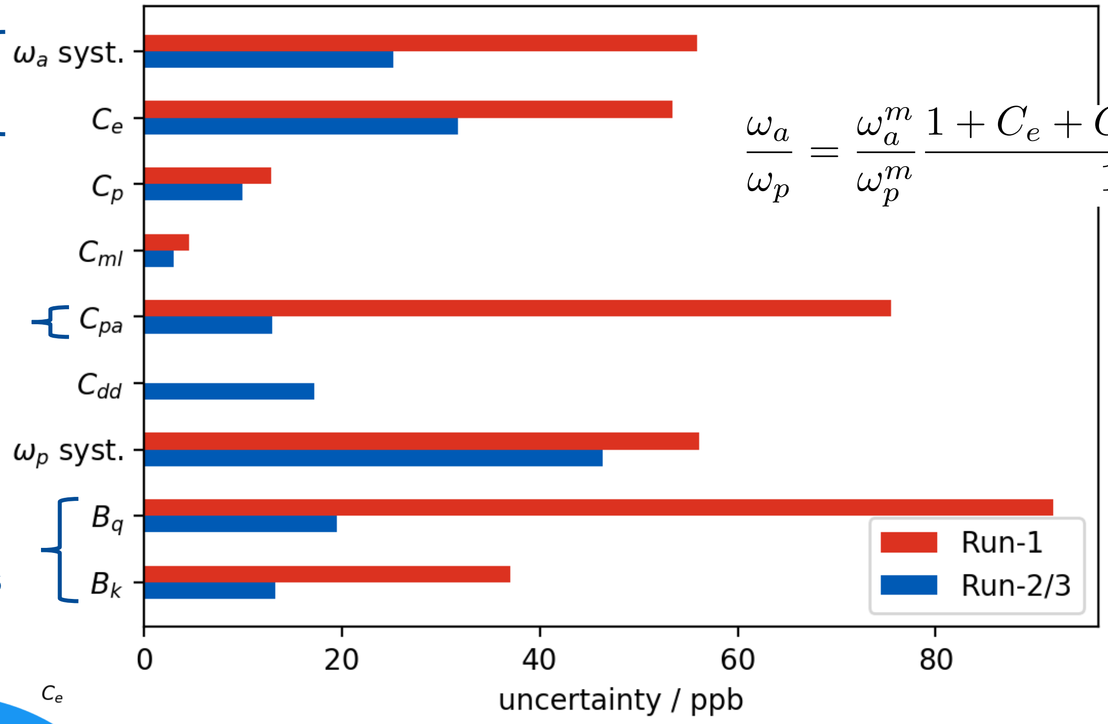

$$\frac{\omega_a}{\omega_p} = \frac{\omega_a^m}{\omega_p^m} \frac{1 + C_e + C_p + C_{pa} + C_{dd} + C_{ml}}{1 + B_k + B_q}$$

157 ppb to 70 ppb

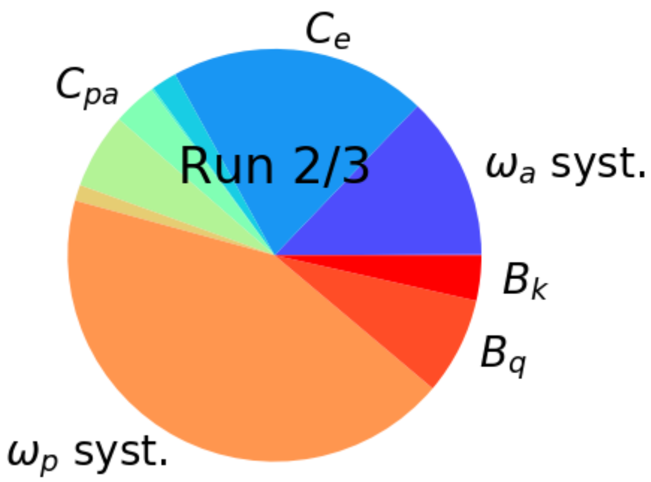

Run-2/3 Publication

Published on PRL – 17th October 2023!

Measurement of the Positive Muon Anomalous Magnetic Moment to 0.20 ppm

D. P. Aguillard,[33] T. Albahri,[30] D. Allspach,[7] A. Anisenkov,[4,a] K. Badgley,[7] S. Baeßler,[35,b] I. Bailey,[17,c] L. Bailey,[27] V. A. Baranov,[15,d] E. Barlas-Yucel,[28] T. Barrett,[6] E. Barzi,[7] F. Bedeschi,[10] M. Berz,[18] M. Bhattacharya,[7] H. P. Binney,[36] P. Bloom,[19] J. Bono,[7] E. Bottalico,[30] T. Bowcock,[30] S. Braun,[36] M. Bressler,[32] G. Cantatore,[12,e] R. M. Carey,[2] B. C. K. Casey,[7] D. Cauz,[26,f] R. Chakraborty,[29] A. Chapelain,[6] S. Chappa,[7] S. Charity,[30] C. Chen,[23,22] M. Cheng,[28] R. Chislett,[27] Z. Chu,[22,g] T. E. Chupp,[33] C. Claessens,[36] M. E. Convery,[7] S. Corrodi,[1] L. Cotrozzi,[10,h] J. D. Crnkovic,[7] S. Dabagov,[8,i] P. T. Debevec,[28] S. Di Falco,[10] G. Di Sciascio,[11] B. Drendel,[7] A. Driutti,[10,h] V. N. Duginov,[15,d] M. Eads,[20] A. Edmonds,[2] J. Esquivel,[7] M. Farooq,[33] R. Fatemi,[29] C. Ferrari,[10,j] M. Fertl,[14] A. T. Fienberg,[36] A. Fioretti,[10,j] D. Flay,[32] S. B. Foster,[2] H. Friedsam,[7] N. S. Froemming,[20] C. Gabbanini,[10,j] I. Gaines,[7] M. D. Galati,[10,h] S. Ganguly,[7] A. Garcia,[36] J. George,[32,k] L. K. Gibbons,[6] A. Gioiosa,[25,l] K. L. Giovanetti,[13] P. Girotti,[10] W. Gohn,[29] L. Goodenough,[7] T. Gorringe,[29] J. Grange,[33] S. Grant,[1,27] F. Gray,[21] S. Haciomeroglu,[5,m] T. Halewood-Leagas,[30] D. Hampai,[8] F. Han,[29] J. Hempstead,[36] D. W. Hertzog,[36] G. Hesketh,[27] E. Hess,[10] A. Hibbert,[30] Z. Hodge,[36] K. W. Hong,[35] R. Hong,[29,1] T. Hu,[23,22] Y. Hu,[22,g] M. Iacovacci,[9,n] M. Incagli,[10] P. Kammel,[36] M. Kargiantoulakis,[7] M. Karuza,[12,o] J. Kaspar,[36] D. Kawall,[32] L. Kelton,[29] A. Keshavarzi,[31] D. S. Kessler,[32] K. S. Khaw,[23,22] Z. Khechadoorian,[6] N. V. Khomutov,[15] B. Kiburg,[7] M. Kiburg,[7,19] O. Kim,[34] N. Kinnaird,[2] E. Kraegeloh,[33] V. A. Krylov,[15] N. A. Kuchinskiy,[15] K. R. Labe,[6] J. LaBounty,[36] M. Lancaster,[31] S. Lee,[5] B. Li,[22,1,p] D. Li,[22,q] L. Li,[22,g] I. Logashenko,[4,a] A. Lorente Campos,[29] Z. Lu,[22,g] A. Lucà,[7] G. Lukicov,[27] A. Lusiani,[10,r] A. L. Lyon,[7] B. MacCoy,[36] R. Madrak,[7] K. Makino,[18] S. Mastroianni,[9] J. P. Miller,[2] S. Miozzi,[11] B. Mitra,[34] J. P. Morgan,[7] W. M. Morse,[3] J. Mott,[7,2] A. Nath,[9,n] J. K. Ng,[23,22] H. Nguyen,[7] Y. Oksuzian,[1] Z. Omarov,[16,5] R. Osofsky,[36] S. Park,[5] G. Pauletta,[26,s] G. M. Piacentino,[25,t] R. N. Pilato,[30] K. T. Pitts,[28,u] B. Plaster,[29] D. Počanić,[35] N. Pohlman,[20] C. C. Polly,[7] J. Price,[30] B. Quinn,[34] M. U. H. Qureshi,[14] S. Ramachandran,[1,k] E. Ramberg,[7] R. Reimann,[14] B. L. Roberts,[2] D. L. Rubin,[6] L. Santi,[26,f] C. Schlesier,[28,v] A. Schreckenberger,[7] Y. K. Semertzidis,[5,16] D. Shemyakin,[4,a] M. Sorbara,[11,w] D. Stöckinger,[24] J. Stapleton,[7] D. Still,[7] C. Stoughton,[7] D. Stratakis,[7] H. E. Swanson,[36] G. Sweetmore,[31] D. A. Sweigart,[6] M. J. Syphers,[20] D. A. Tarazona,[6,30,18] T. Teubner,[30] A. E. Tewsley-Booth,[29,33] V. Tishchenko,[3] N. H. Tran,[2,x] W. Turner,[30] E. Valetov,[18] D. Vasilkova,[27,30] G. Venanzoni,[30,l] V. P. Volnykh,[15] T. Walton,[7] A. Weisskopf,[18] L. Welty-Rieger,[7] P. Winter,[1] Y. Wu,[1] B. Yu,[34] M. Yucel,[7] Y. Zeng,[23,22] and C. Zhang[30]

(The Muon $g-2$ Collaboration)

PhysRevLett.131.161802

Quantity	Correction (ppb)	Uncertainty (ppb)
ω_a^m (statistical)	···	201
ω_a^m (systematic)	···	25
C_e	451	32
C_p	170	10
C_{pa}	−27	13
C_{dd}	−15	17
C_{ml}	0	3
$f_{\text{calib}} \cdot \langle \omega'_p(\vec{r}) \times M(\vec{r}) \rangle$	···	46
B_k	−21	13
B_q	−21	20
$\mu'_p(34.7°)/\mu_e$	···	11
m_μ/m_e	···	22
$g_e/2$	···	0
Total systematic for $\mathcal{R}'_\mu$	···	70
Total external parameters	···	25
Total for a_μ	622	215

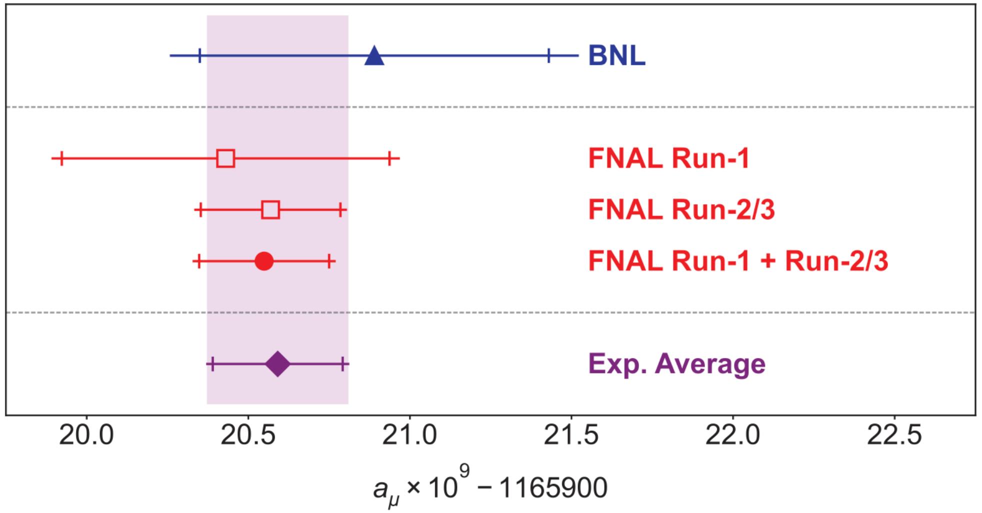

Theory comparison – The puzzle

- Theory prediction is less clear now.
- Comparing with WP (2020) a large discrepancy is found **5.0σ**

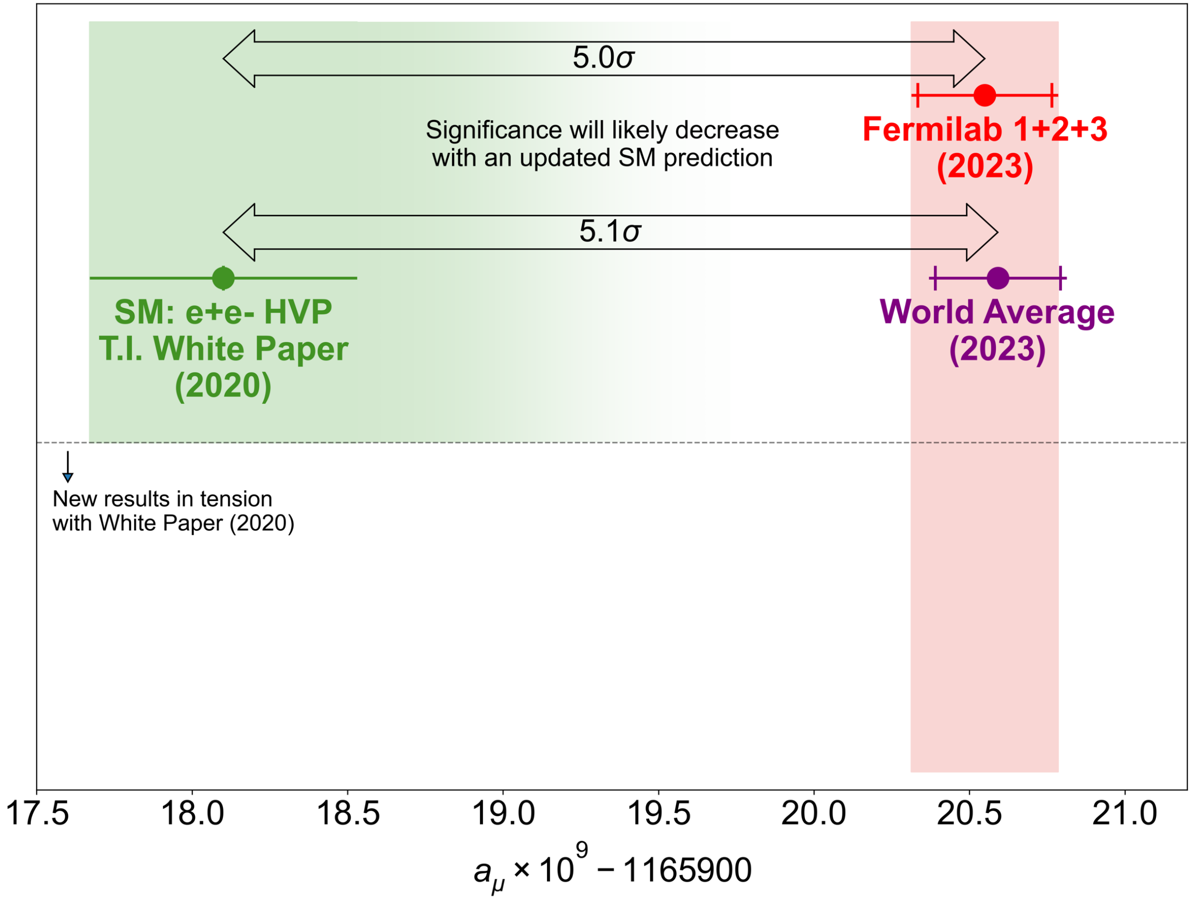

Theory comparison – The puzzle in the puzzle

- Theory prediction is less clear now.
- Comparing with WP (2020) a large discrepancy is found **5.0σ**

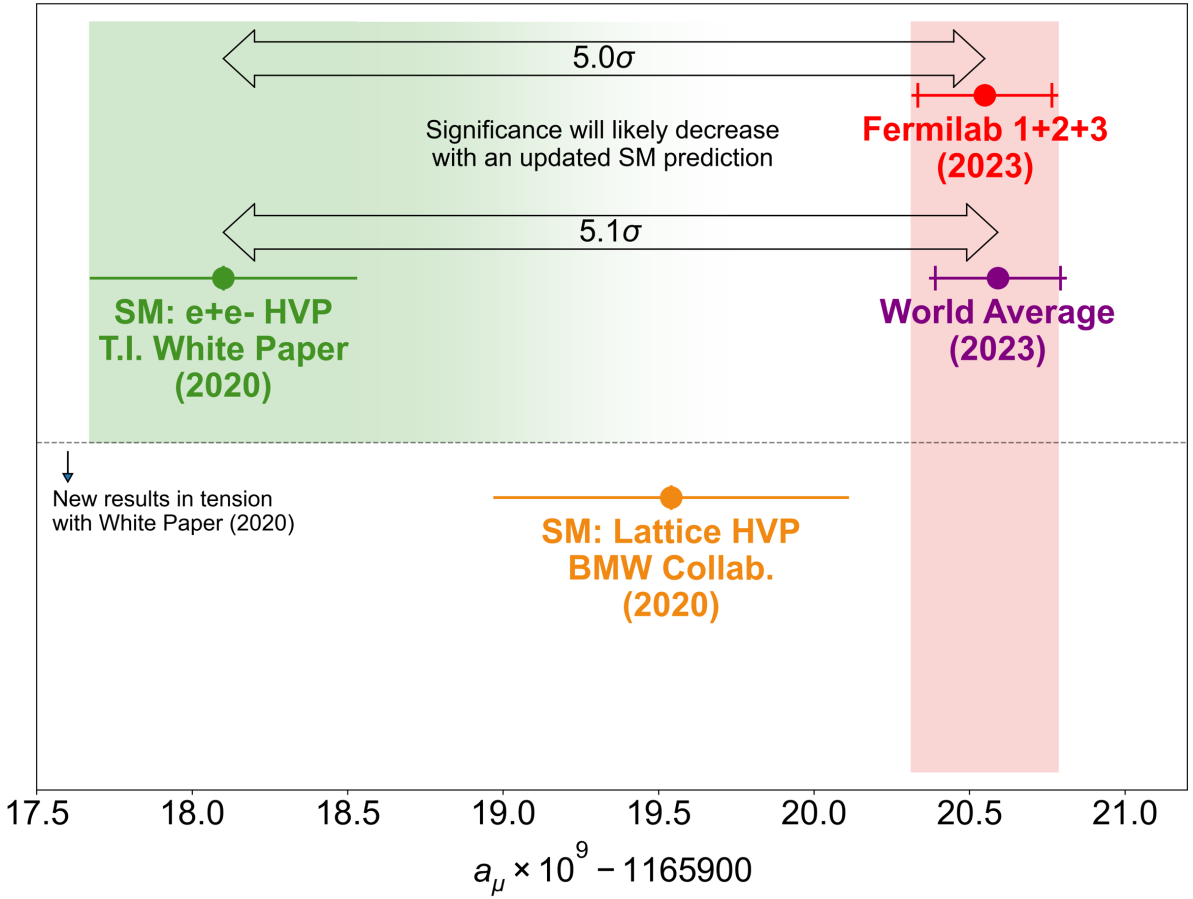

- Considering **BMW** result for the HVP term, instead of WP the discrepancy is reduced.

Theory comparison – The puzzle^3

- New results from **SND2k** and **CMD-3** since White Paper, **CMD-3** shows a discrepancy.
- From lattice side, other groups are improving the precision of the calculation, converging on a common value.

Dispersive Approach

Keshavarzi, Nomura, Teubner: Priv. Comm.

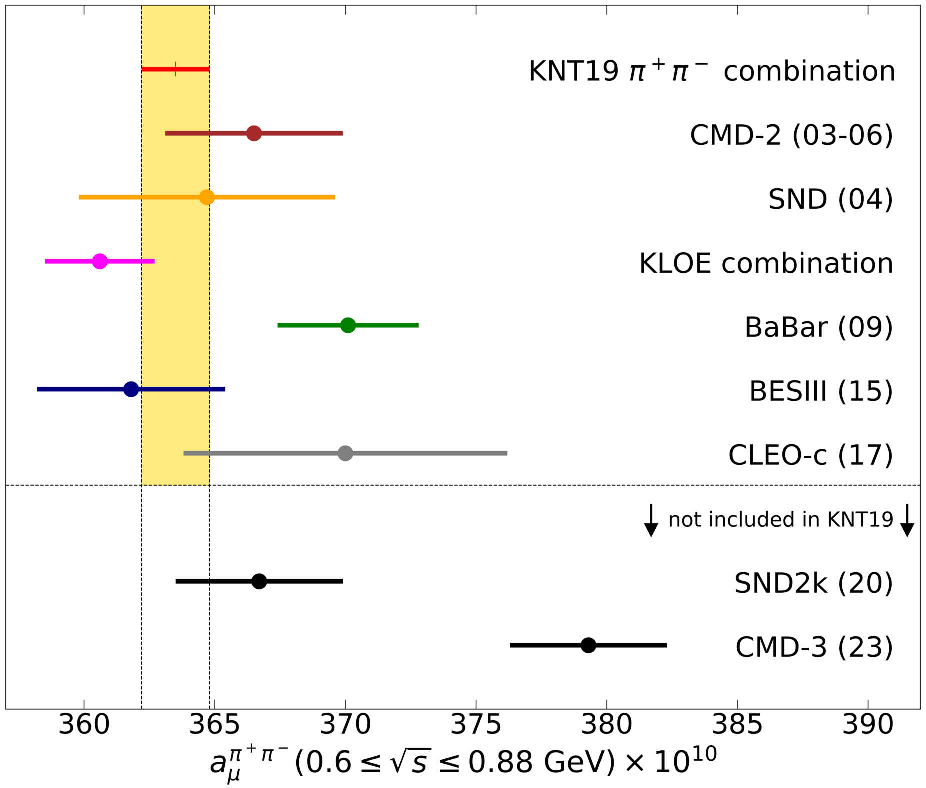

Lattice QCD Approach

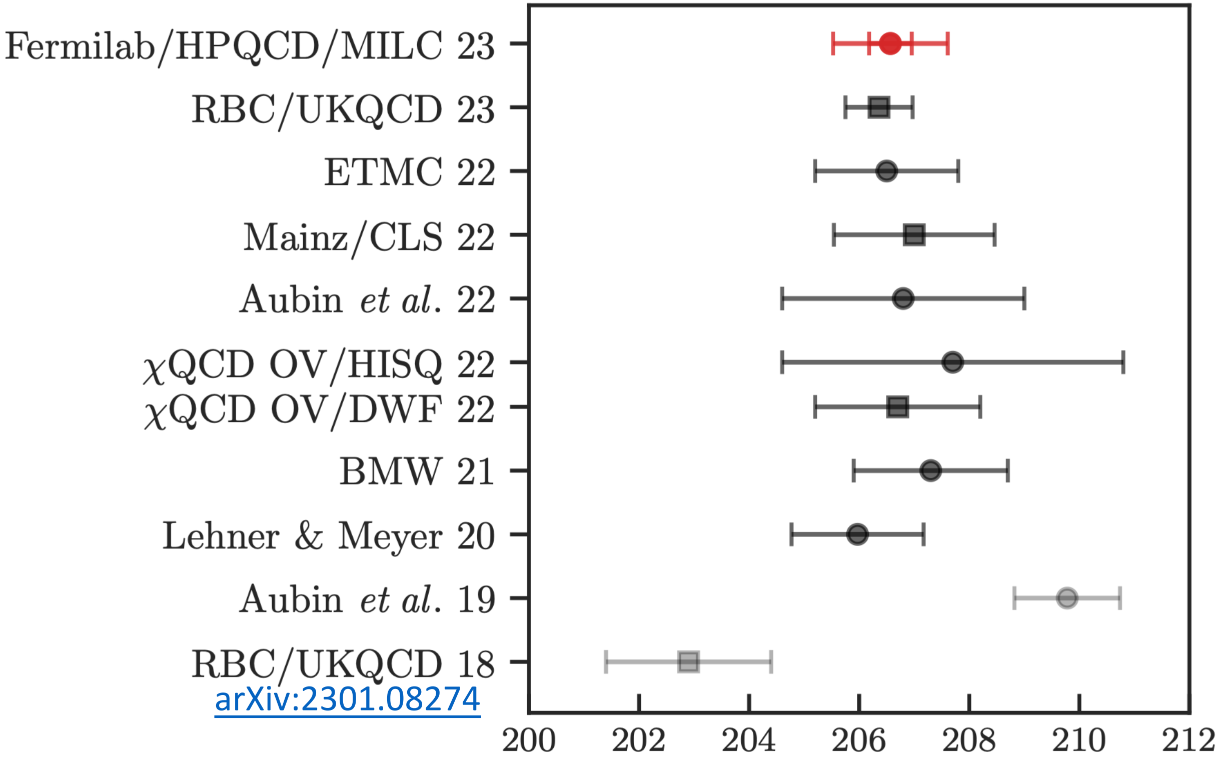

arXiv:2301.08274

Muon *g*-2 - Run-4/5/6 further improvements

- During Run-4, the quadruple **RF dampening system** has been installed and tuned.
- In Run-5 the RF has been used for production data, in order to **reduce radial oscillation of the beam**

CBO amplitude: factor of 8.6
5.3 → 0.6 mm (for 30-50 us fit)

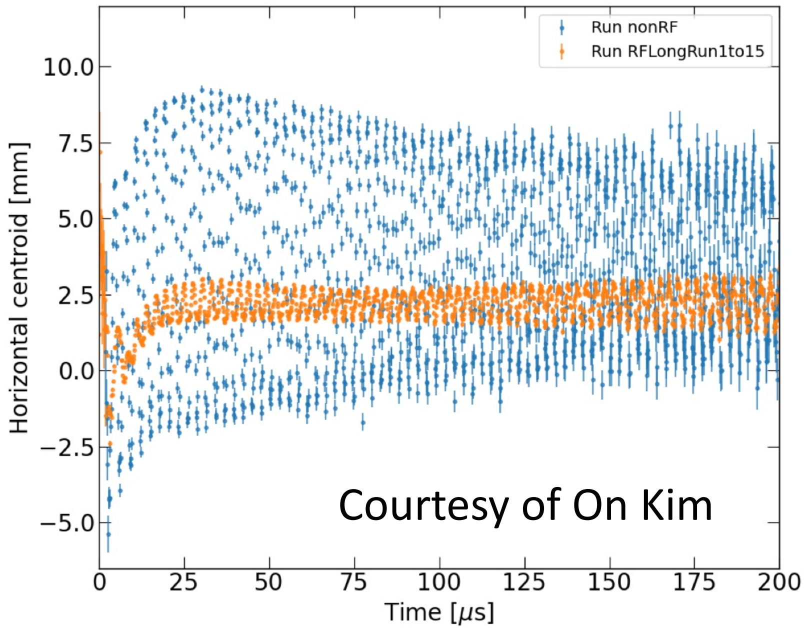

- During Run-5/6 has been installed a **Mini**mally intrusive **Sci**ntillating **Fi**ber detector (**MiniSciFi**) useful to measure the time momentum correlation for E-field correction and the CBO oscillation.

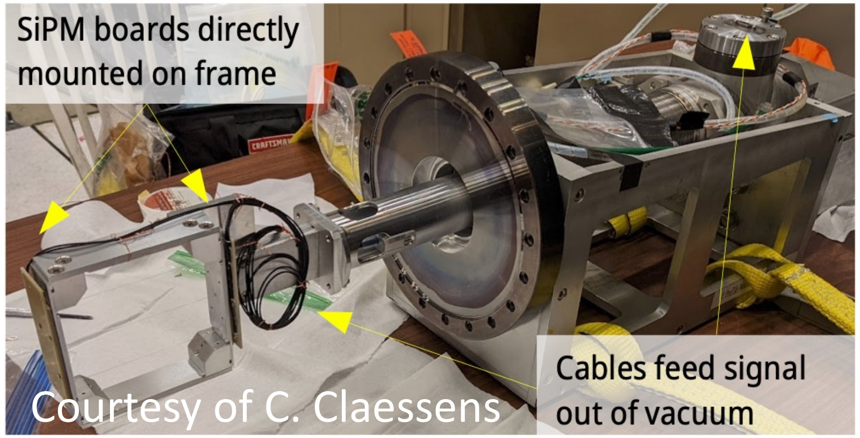

Muon *g*-2 Outlook

- The data **acquisition** is **finished** on **9th July 2023**.
- We reached the TDR goal of **21 BNL** on **27th February 2023**.
- Run-4/5/6 result is expected in ~**2025**.

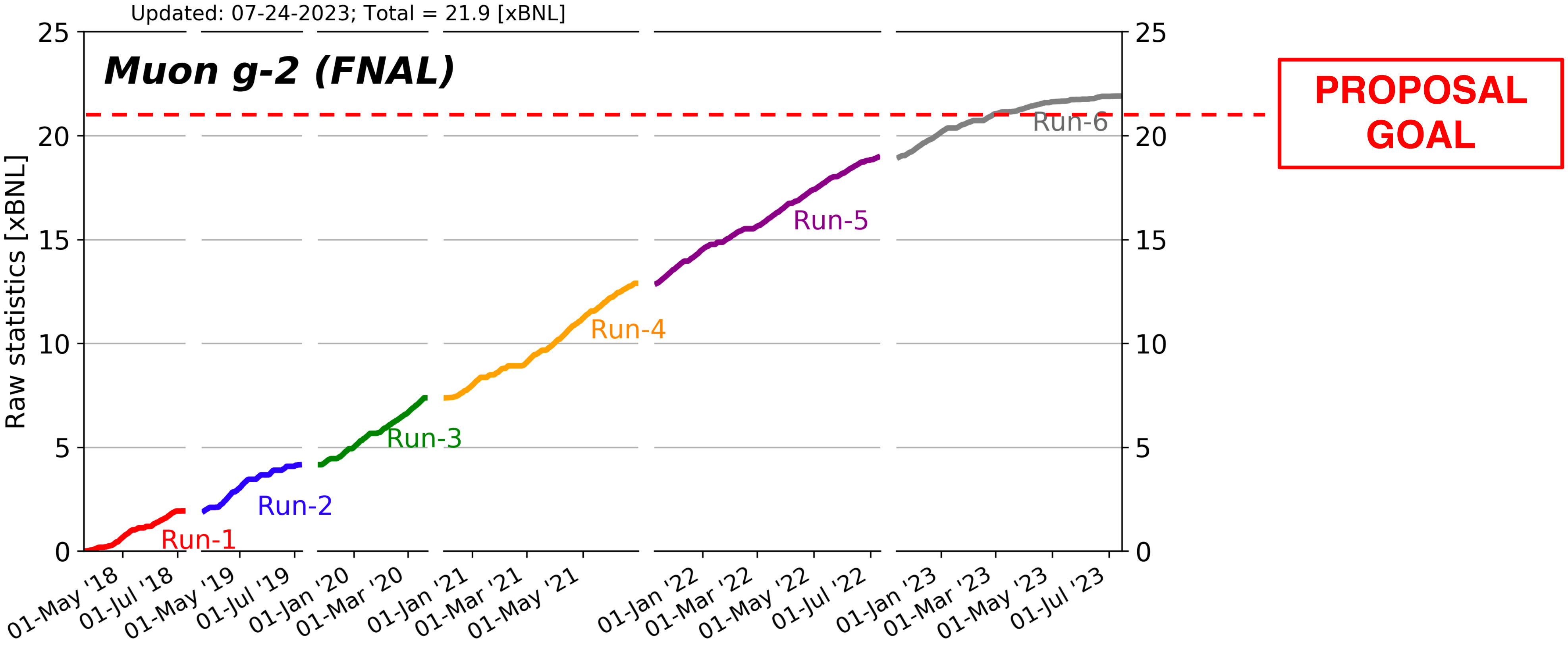

Conclusion

- We've determined a_μ to an unprecedented **203 ppb** precision

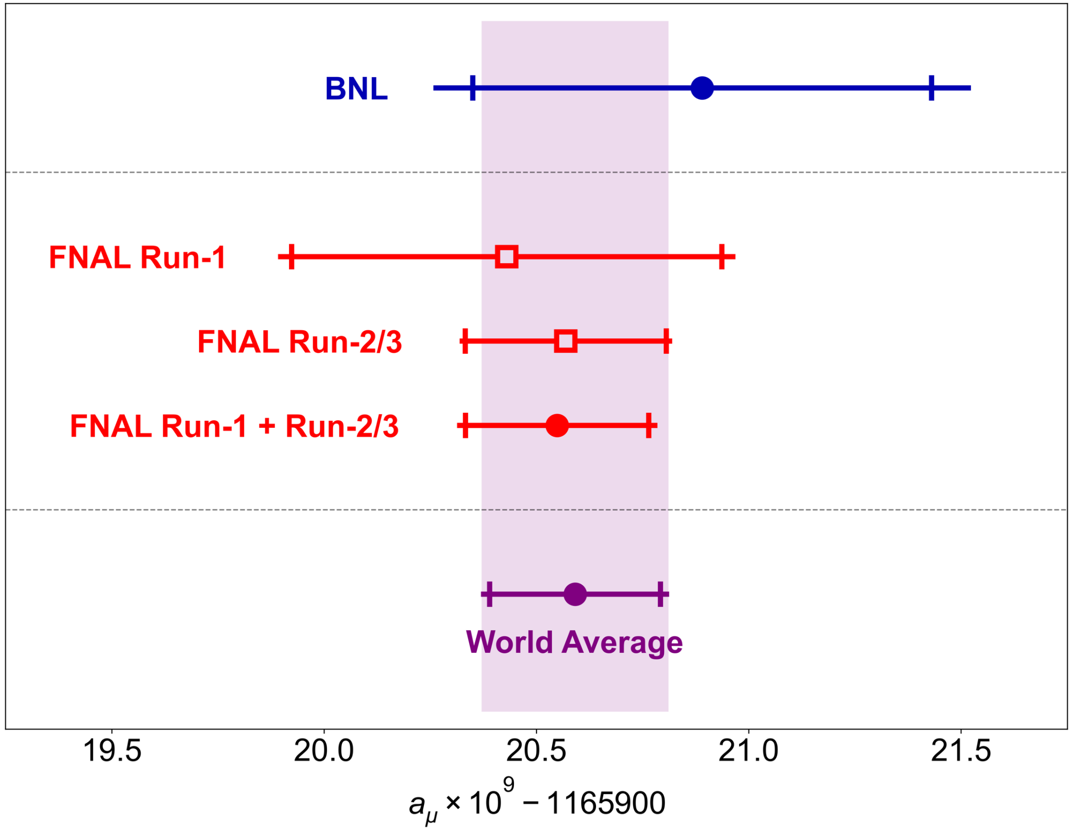

New result is in **excellent agreement with Run-1 & BNL**

More than **halved the total uncertainty** from Run-1

Improved our design goal with systematic uncertainty of **70 ppb**.

- There is **more data** to analyze and we'll squeeze uncertainty down further in our future results!

“The closer you look the more there is to see”

F. Jegerlehner

Thank you!!!

- For any question or just to have a chat – elia.bottalico@liverpool.ac.uk

BACK-UP

Kickers and Inflector

- The **inflector** cancels the storage ring field such that the muons are not deflected by the main **1.45 T** field.
- Superconducting, operational current ~2.6 kA.

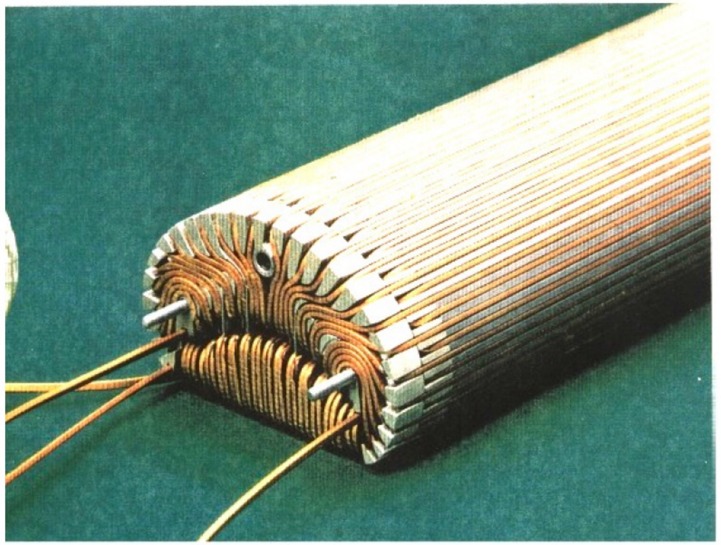

- **3 Kickers** are necessary to inject magic momentum muons along the magic radius (7.11 m) with a required kick at order of 10 mrad.
- 4 kA current in 200 ns pulse.
- Design kick strength has been reached in Run-3 (~160 kV).

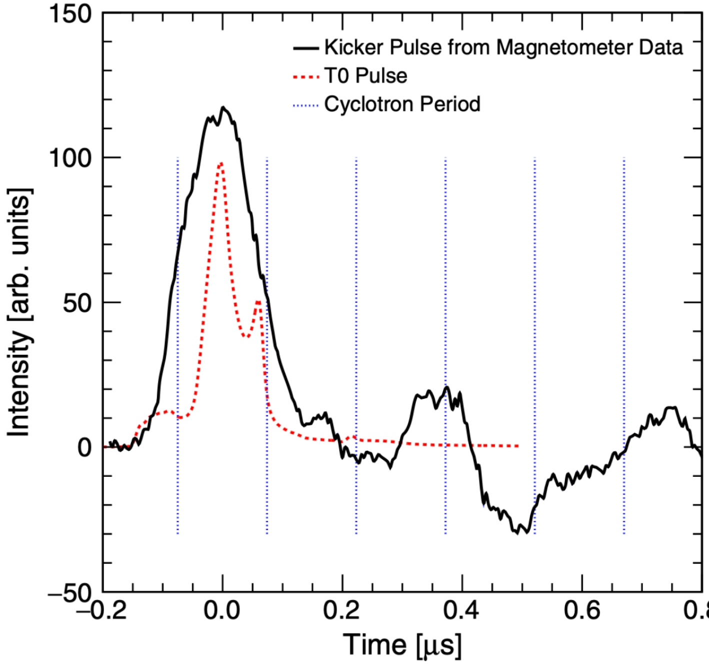

Quadrupoles

- The Electrostatic Quadrupoles (ESQ) system allows to strongly focus the beam vertically, four ESQ stations are symmetrically placed around the ring.
- The plates are raised from ground to operating voltage prior to each *fill* with RC charging time constants of **$\sim 5\ \mu s$**.
- This procedure, known as **scraping**, initially displaces the beam vertically and horizontally with respect to the central closed orbit.

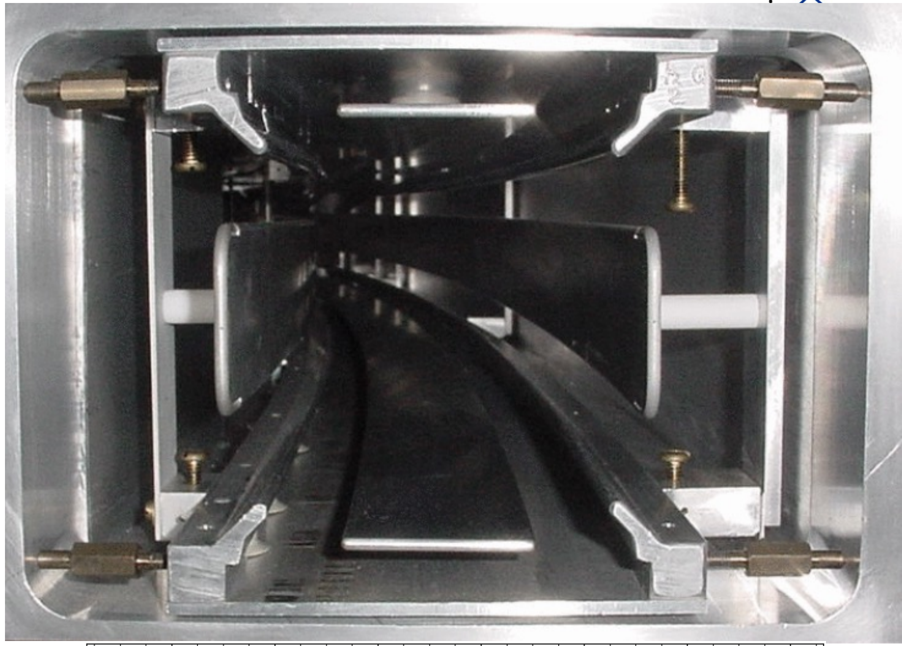

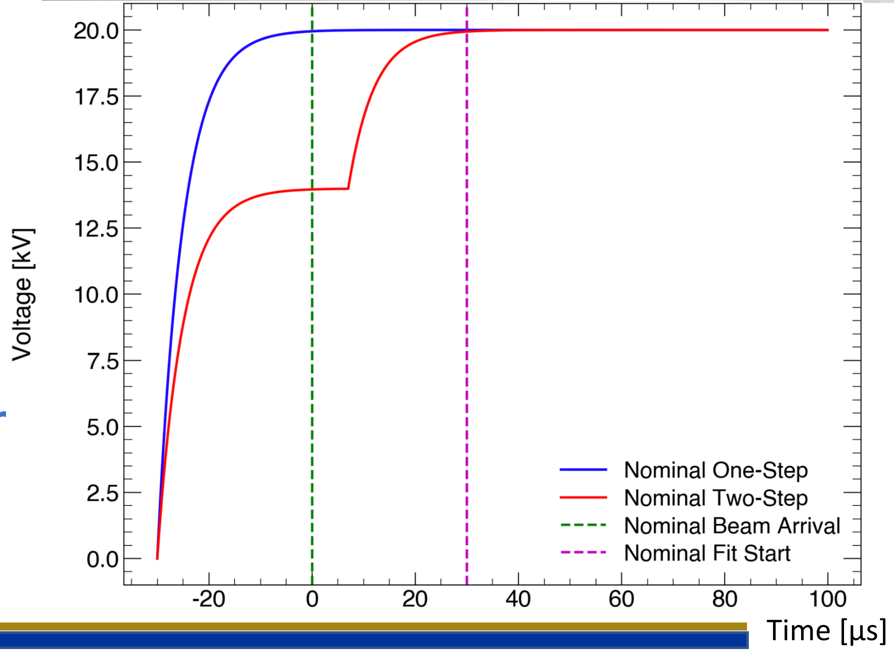

ω_a measurement – CBO oscillation

- Given the restoring force by radial magnetic field, the beam oscillates radially (vertically too) as the betatron frequency: $\omega_{BO} = \omega_c\sqrt{1-n}$, where $\boldsymbol{n}$ is the field-index.
- The beam is measured by detectors, calorimeters and trackers.
- The $\omega_{BO} < \omega_C$, so calorimeters see a different phase at each turn, measuring an oscillation called **Coherent Betatron Oscillation** (**CBO**), given by $\omega_{CBO} = \omega_C - \omega_{BO}$

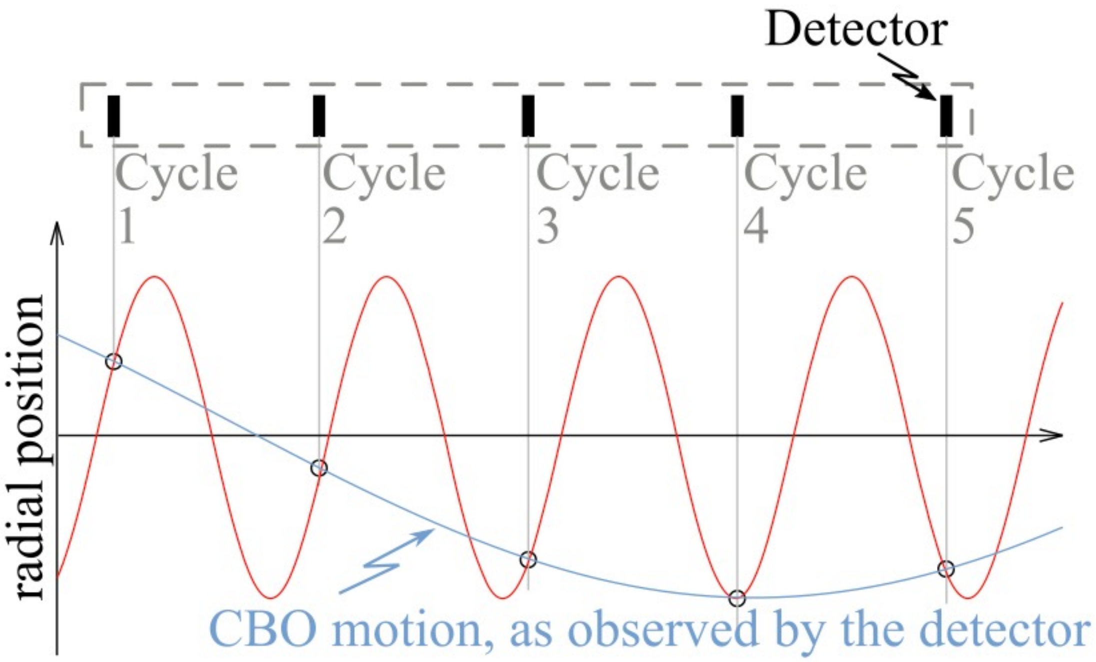

$$2\pi f_{CBO} = \omega_C - \omega_{BO} = \omega_C(1-\sqrt{1-n})$$

$$\omega_{CBO} = 2.34\, rad/\mu s$$

Where $T_C \sim 0.149\, ns$ and $n \sim 0.108$

Beam dynamics correction to ω_a: C_e

Considering the extended expression of the spin precession frequency in a magnetic field:

$$\overrightarrow{\omega_a} = \frac{e}{m}\left[a_\mu \vec{B} - \left(a_\mu - \frac{1}{\gamma^2 - 1}\right)(\vec{\beta}\times\vec{E}) - a_\mu\left(\frac{\gamma}{\gamma+1}\right)(\vec{\beta}\cdot\vec{B})\vec{\beta}\right]$$

This term introduces a bias on ω_a that needs to be corrected by Electric Field correction:

$C_e = 2n(1-n)\beta^2 \frac{<x_e^2>}{R_0^2}$ is proportional to the equilibrium radius distribution x_e.

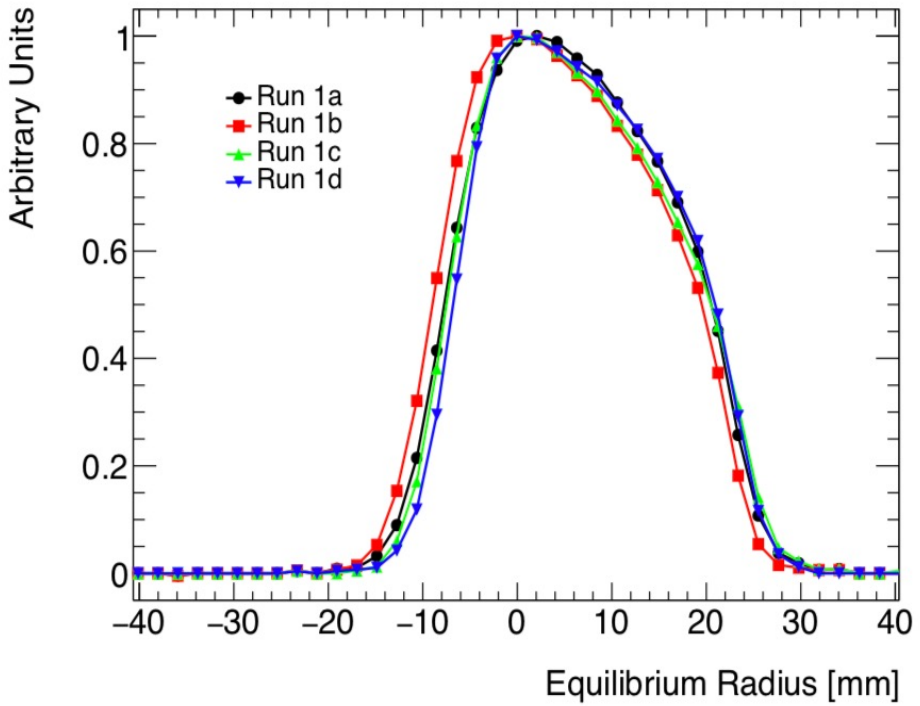

$$C_e \sim 489\ ppb$$

Beam dynamics correction to $\boldsymbol{\omega_a}$: C_p

Considering the extended expression of the spin precession frequency in a magnetic field:

$$\overrightarrow{\omega_a} = \frac{e}{m}\left[a_\mu \vec{B} - \left(a_\mu - \frac{1}{\gamma^2 - 1}\right)(\vec{\beta}\times\vec{E}) - a_\mu\left(\frac{\gamma}{\gamma + 1}\right)(\vec{\beta}\cdot\vec{B})\vec{\beta}\right]$$

$$C_p \sim 200\, ppb$$

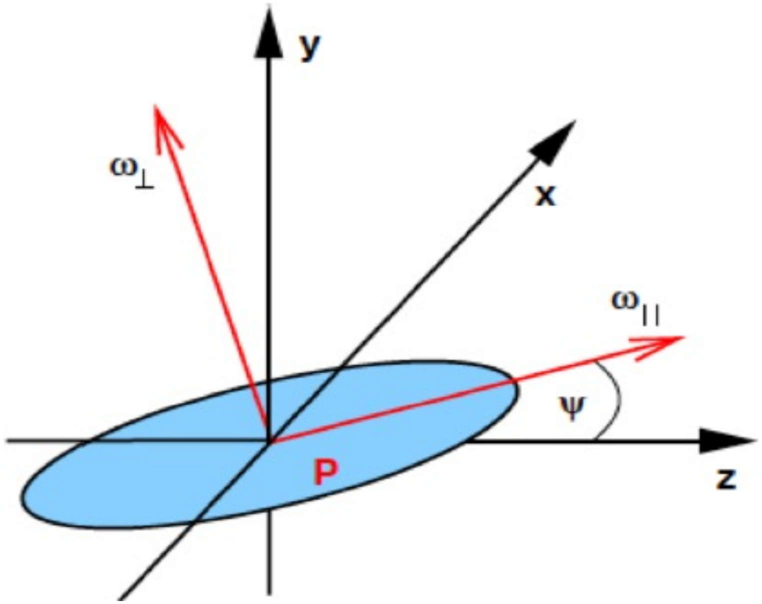

$\boldsymbol{C_p}$: the pitch correction $C_p = n < A_y^2 > /4R_0^2$ depends on amplitude vertical oscillation (A_y).

a_μ systematic sources

Many systematics come from effects that **change** the **phase** of the detected positrons **over time** and introduce a bias on ω_a:

$$cos(\omega_a t + \phi(t)) = cos(\omega_a t + \phi_0 + \phi' t + ...)$$
$$= cos((\omega_a + \phi')t + \phi_0 + ...)$$

In general, anything that changes from **early-to-late** within each muon fill can be a cause of systematic error, as:

- Beam distortion
- Muon losses
- Varying lifetime
- Rate dependent reconstruction

Beam dynamics correction to $\boldsymbol{\omega_a}$: C_{lm}

$\boldsymbol{C_{lm}}$: describes the motion introduced on ω_a phase due to the loss of muon during the *fill*. It's explained by:

1. Muons with different momentum have different phase;
2. The number of loss muon change as function of momentum.

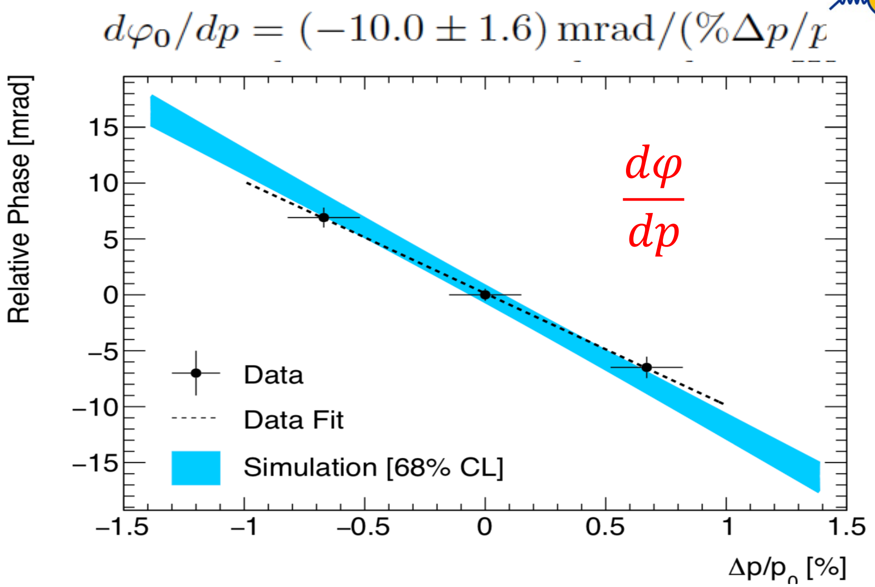

1) 2)

$$\Delta\omega_a = \frac{d\varphi}{dt} = \frac{d\varphi}{dp} \cdot \frac{dp}{dt}$$

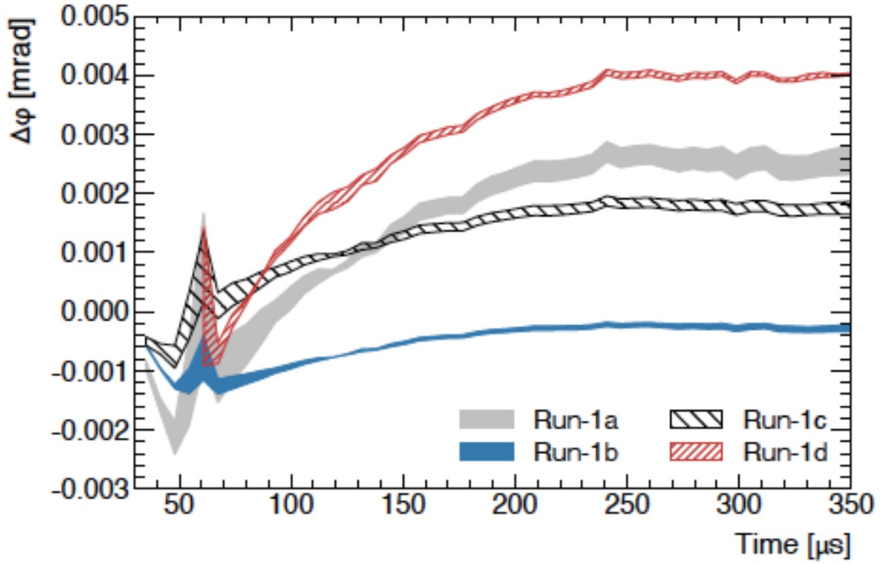

$$C_{lm} < 20\ ppb$$

Beam dynamics correction to ω_a: C_{pa}

- The measured *g-2* phase of the muon is decay vertex position dependent.
- It is obtained as weighted average of the phases measured by each (x,y) pair position.

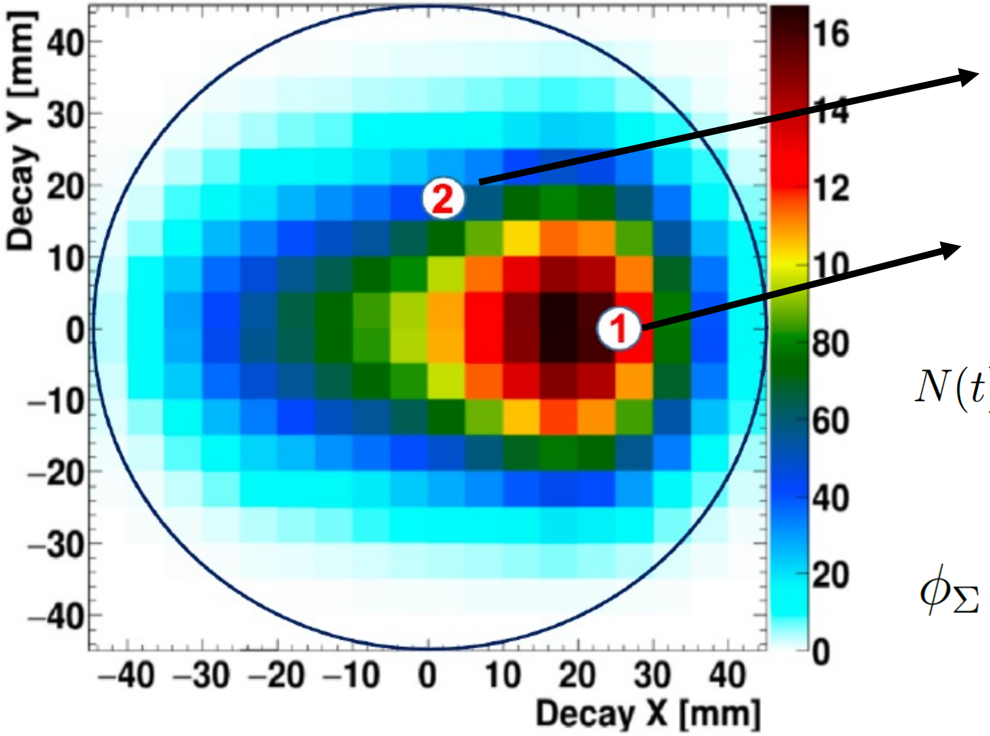

$$N_2(t) = N_{02}e^{-t/\tau}\left[1 + A_2\cos(\omega_a t + \phi_2)\right]$$

$$N_1(t) = N_{01}e^{-t/\tau}\left[1 + A_1\cos(\omega_a t + \phi_1)\right]$$

$$N(t) = N_1(t) + N_2(t) = N_\Sigma e^{-t/\tau}\left[1 + A_\Sigma\cos(\omega_a t + \phi_\Sigma)\right]$$

$$\phi_\Sigma = \arctan\frac{N_{01}A_1\sin(\phi_1) + N_{02}A_2\sin(\phi_2)}{N_{01}A_1\cos(\phi_1) + N_{02}A_2\cos(\phi_2)}$$

Phase acceptance: Beam Motion Effects

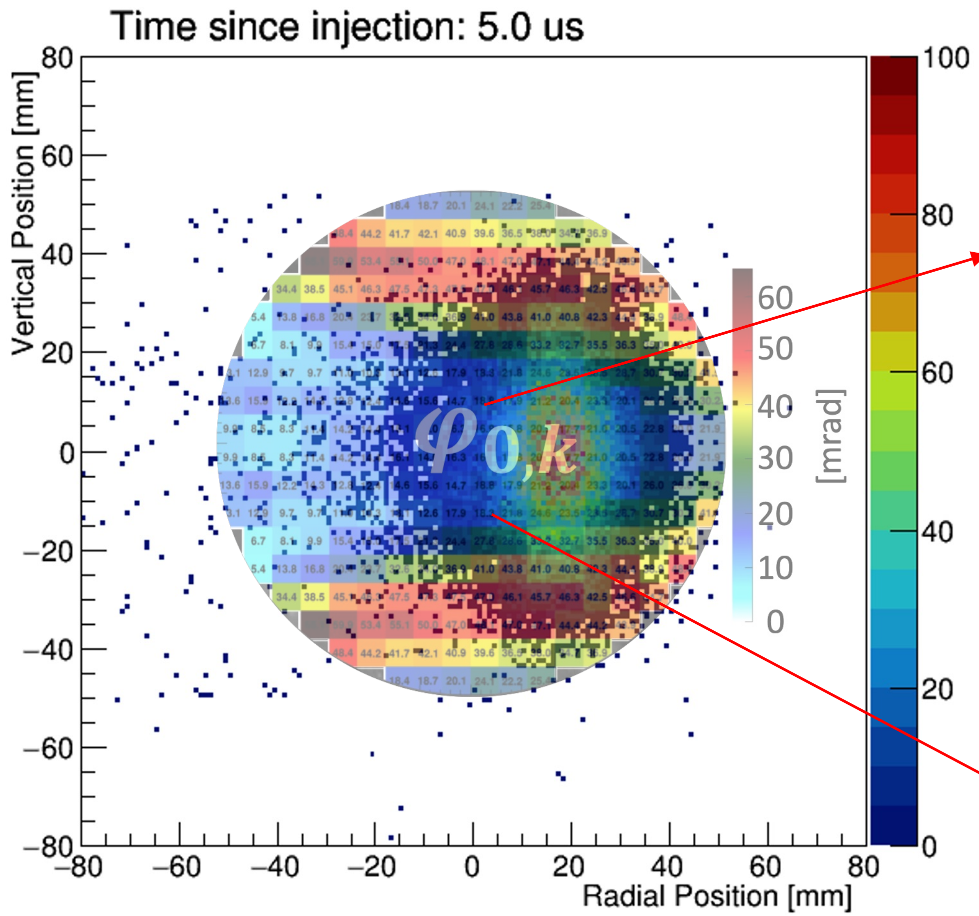

VERTICAL WIDTH VARIATION

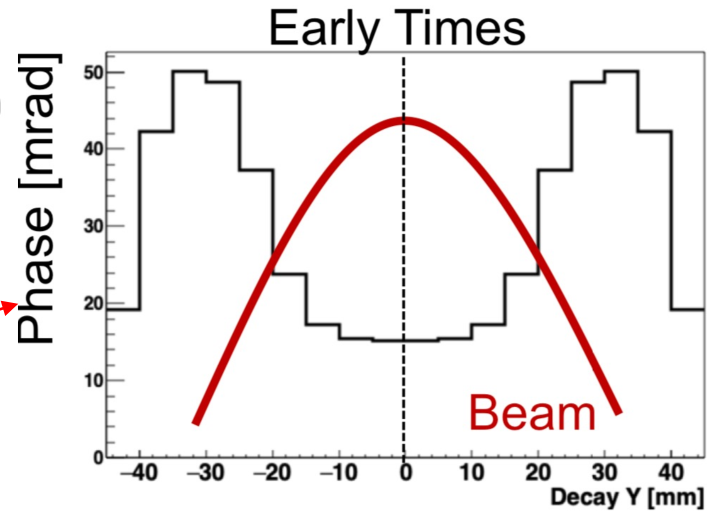

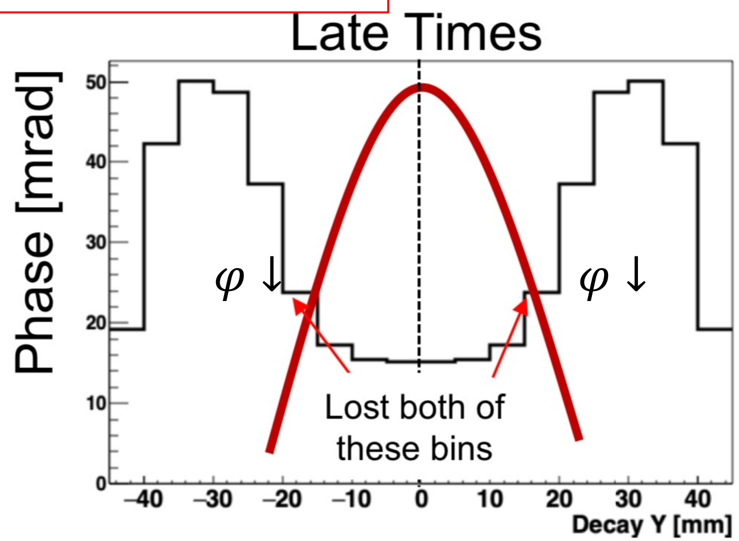

RADIAL MEAN VARIATION

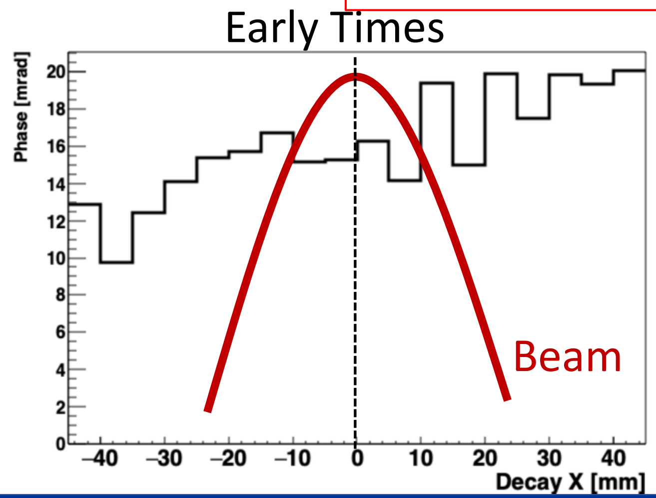

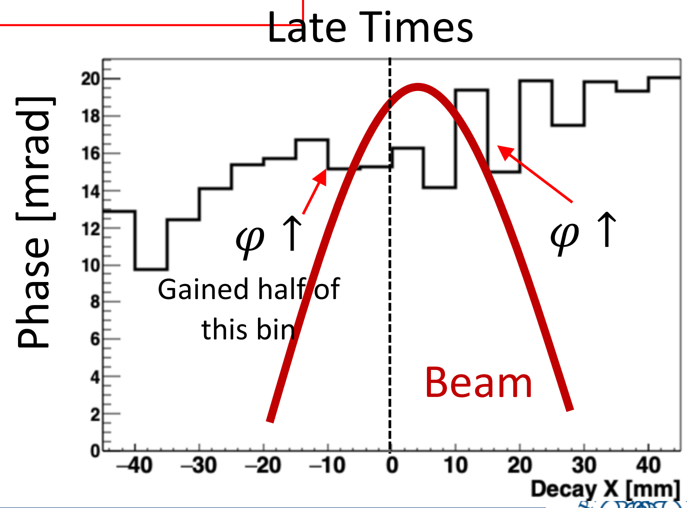

Beam dynamics correction to $\boldsymbol{\omega_a}$: C_{pa}

$\boldsymbol{C_{pa}}$: it is a Phase Acceptance effect. It is due to:

1. Beam variation during the *fill;*
2. Phase measured as function of the decay position.

$$\Delta\omega_a = \frac{d\varphi}{dt} = \underbrace{\frac{dY_{RMS}}{dt}}_{1)} \cdot \underbrace{\frac{d\varphi}{dY_{RMS}}}_{2)}$$

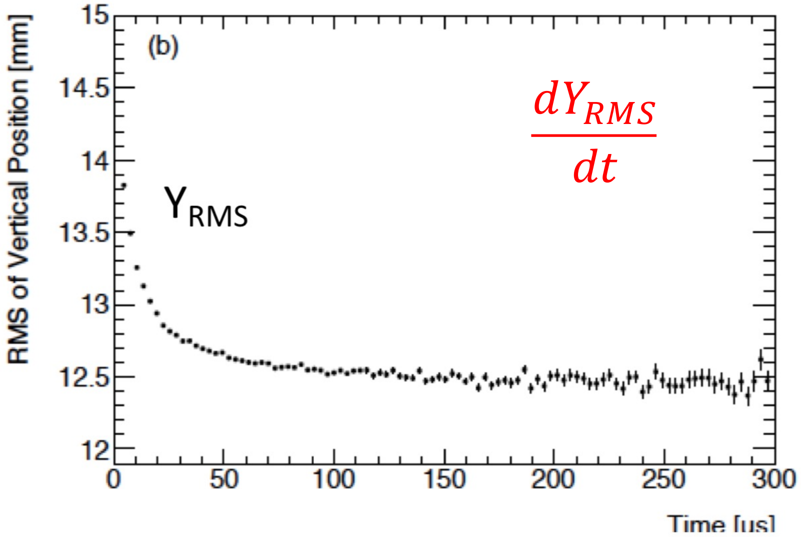

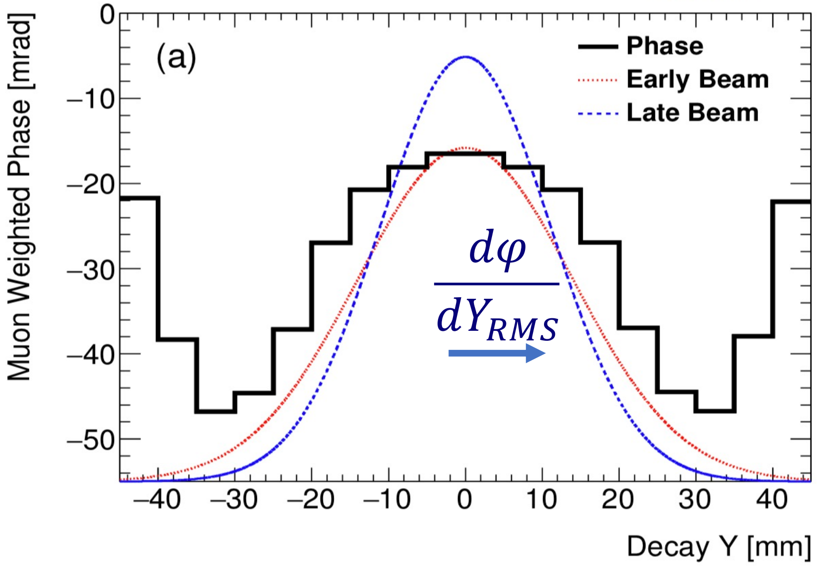

The effect was large in Run1 due to *broken resistors*

$$\boxed{C_{pa} \sim 180\ ppb}$$

We expect a reduction in Run2/3 (~50ppb/ ~20ppb)

Beam dynamics correction to ω_a

- These are the results for the BD corrections from Run-1, the **phase acceptance** (C_{pa}) correction was one of the topic I addressed during my PhD.
- Now analysis is ongoing to finalize the Run-2/3 beam dynamics corrections, stay tuned!

	Correction Factor [ppb]	Uncertainty [ppb]
ω_a (stat.)	–	434
ω_a (syst.)	–	56
f_b/f_0	–	2
C_e	489	53
C_p	180	13
C_{ml}	−11	5
C_{pa}	−158	75
$f_{calib}\ \langle \omega'_p(x,y,\phi) \cdot M(x,y,\phi) \rangle$	–	56
B_q	−17	92
B_k	−27	37
$\mu'_p(34.7^\circ C)/\mu_e$ [PCK77]	–	10
m_μ/m_e [LAMPF-99; CD-2018]	–	22
$g_e/2$ [HFG08]	–	0
Total Systematic	–	157
Total Fundamental Factors	–	25
Total	544	461